TURUN YLIOPISTON JULKAISUJA
ANNALES UNIVERSITATIS TURKUENSIS

SARJA - SER. A I OSA - TOM. 393

ASTRONOMICA - CHEMICA - PHYSICA - MATHEMATICA

DESIGN AND PRODUCTION OF PROTEIN NANOSTRUCTURES FOR BIOMOLECULAR DETECTION

by

Anu Jääskeläinen

TURUN YLIOPISTO
Turku 2009

From
Department of Biochemistry and Food Chemistry
University of Turku
Turku, Finland

Supervised by
Professor Marko Virta, PhD
Department of Applied Chemistry and Microbiology
University of Helsinki
Helsinki, Finland

Professor Tero Soukka, PhD
Department of Biochemistry and Food Chemistry / Biotechnology
University of Turku
Turku, Finland

Professor Lauri J. Pelliniemi, MD
Institute of Microbiology and Pathology / Electron Microscopy
University of Turku
Turku, Finland

Reviewed by
Professor Pirkko Heikinheimo, PhD
Institute of Biotechnology
University of Helsinki
Helsinki, Finland

Per Matsson, PhD
Phadia AB
Associate Professor
University of Uppsala
Uppsala, Sweden

Opponent
Professor François Baneyx, PhD
Department of Chemical Engineering
University of Washington
Seattle, WA, USA

ISBN 978-951-29-3905-3 (PRINT)
ISBN 978-951-29-3906-0 (PDF)
ISSN 0082-7002
Painosalama Oy – Turku, Finland 2009


Isille, Äitille, Suville,
Mummille(†), Sannille,
Sakelle, Pinksille,
Leeville

”Sitä joko jaksaa tai murenee…”

-Kummeli

Table of contents

List of original publications

This thesis is based on the following publications:

I. Production of apoferritin-based bioinorganic hybrid nanoparticles by bacterial fermentation followed by self-assembly. Small. 2007 Aug;3(8):1362-7.

II. Biologically produced bifunctional recombinant protein nanoparticles for immunoassays. Anal Chem. 2008 Feb 1;80(3):583-7.

III. Development of a denaturation/renaturation-based production process for ferritin nanoparticles. Biotechnol Bioeng. 2008 Mar 1;102(4):1012-24.

IV. Biological production of protein-based particles for particle-enhanced agglutination assays. Manuscript submitted for publication.

Abbreviations

αTSH	Anti-TSH antibody
BCCP	Biotin carboxyl carrier protein
CBP	Calmodulin binding peptide
cDNA	Complementary DNA
CV	Coefficient of variation
Dpr	Dps-like peroxide resistance
Dps	DNA-binding proteins during stationary phase
DTPA	Diethylenetriamine pentaacetic acid
E. coli	*Escherichia coli*
Flp	Ferritin-like protein
GEPI	Genetically engineered peptide for inorganics
kDa	Kilo Dalton
MRI	Magnetic resonance imagining
PAGE	Polyacrylamide gel electrophoresis
PCR	Polymerase chain reaction
PEG	Polyethylene glycol
RFU	Relative fluorescence unit
SA	Streptavidin
S. cerevisiae	*Saccharomyces cerevisiae*
scFv	Single chain Fv antibody fragment
SCID	Severe combined immunodefiency
SDS	Sodium dodecyl sulfate
SNP	Single nucleotide polymorphism
TEM	Transmission electron microscopy
TSH	Thyroid stimulating hormone
TRF	Time-resolved fluorometry
UV	Ultraviolet

Abstract

Particulate nanostructures are increasingly used for analytical purposes. Such particles are often generated by chemical synthesis from non-renewable raw materials. Generation of uniform nanoscale particles is challenging and particle surfaces must be modified to make the particles biocompatible and water-soluble. Usually nanoparticles are functionalized with binding molecules (*e.g.*, antibodies or their fragments) and a label substance (if needed). Overall, producing nanoparticles for use in bioaffinity assays is a multistep process requiring several manufacturing and purification steps.

This study describes a biological method of generating functionalized protein-based nanoparticles with specific binding activity on the particle surface and label activity inside the particles. Traditional chemical bioconjugation of the particle and specific binding molecules is replaced with genetic fusion of the binding molecule gene and particle backbone gene. The entity of the particle shell and binding moieties are synthesized from generic raw materials by bacteria, and fermentation is combined with a simple purification method based on inclusion bodies. The label activity is introduced during the purification. The process results in particles that are ready-to-use as reagents in bioaffinity. Apoferritin was used as particle body and the system was demonstrated using three different binding moieties: a small protein, a peptide and a single chain Fv antibody fragment that represents a complex protein including disulfide bridge. If needed, Eu^{3+} was used as label substance.

The results showed that production system resulted in pure protein preparations, and the particles were of homogeneous size when visualized with transmission electron microscopy. Passively introduced label was stably associated with the particles, and binding molecules genetically fused to the particle specifically bound target molecules. Functionality of the particles in bioaffinity assays were successfully demonstrated with two types of assays; as labels and in particle-enhanced agglutination assay.

This biological production procedure features many advantages that make the process especially suited for applications that have frequent and recurring requirements for homogeneous functional particles. The production process of ready, functional and water-soluble particles follows principles of “green chemistry”, is upscalable, fast and cost-effective.

1 Introduction

Submicrometer-sized nanoparticles have been developed for bioaffinity assays used to quantify the presence of specific molecules from various samples. Such particles are typically employed as labels in diverse assay formats and as enhancers in agglutination-based assays, and also, to some extent, as solid phases. Various luminescent, fluorescent, semiconducting, electrochemical and magnetic nanosized particles have been used as labels in different detection technologies (Chan and Nie, 1998; Härmä *et al.*, 2001; Schultz *et al.*, 2000; Wang *et al.*, 2003; Zijlmans *et al.*, 1999). In general, nanoparticles offer specific activities superior to those of conventional labels (Soukka *et al.*, 2001) and label-particle-related research is vigorous. In particle-enhanced agglutination assays, nanometer-scale particles are agglutinated in the presence of target molecules and the induced light dispersion is detected by turbidometry or nephelometry.

The preparation of functionalized nanoparticles for biological detection applications usually consists of several distinct production and purification steps, each requiring control of the quality. Particles are synthesized using organic or inorganic processes, and when separate label molecules or ions are needed they are introduced either during particle synthesis or afterwards. Additionally, binding molecules, such as antibodies, must be separately produced, usually in biological processes such as cell culture (eukaryotic or prokaryotic) or animal immunization, and then isolated and purified. Bioconjugation to nanoparticles is performed actively (*i.e.*, by forming covalent bonds via chemical reactions) or passively (*i.e.*, by hydrophobic and/or electrostatic adsorption), after which unbound excess binding molecules must be separated from the particles. Conjugation often occurs in random orientations resulting in loss of a considerable proportion of binding capacity.

Particles employed in bioaffinity assays are often of organic polymer nature, such as polystyrene or copolymers thereof generated by chemical synthesis. In addition, inorganic metallic particles have generated interest because of inherent features exceptionally valuable in nanoelectronic and biological applications. The generation of uniform nanoscale particles is challenging, and the characteristics of both organic and inorganic particles are not optimal for use under biological conditions. Often, particle surfaces must be modified to make the particles biocompatible and water-soluble (Dubertret *et al.*, 2002; Matsuya *et al.*, 2003), and also to enable conjugation of biological binding molecules. Particle biocompatibility is an important issue in biological assays; biocompatibility improves the solubility of particulate reagents and minimizes both particle aggregation and nonspecific interactions between sample components and assay reagents.

The concept of green chemistry *i.e.*, sustainable chemistry is one important aspect in contemporary chemistry and especially in nanotechnology. The principles of green chemistry include twelve items (U.S. Environmental Protection Agency): (1) Prevent waste that need to be treated. (2) Design safer chemicals and products. (3) Design less hazardous chemical syntheses. (4) Use renewable feedstock. (5) Use catalysts. (6) Avoid chemical derivatives. (7) Maximize atom economy. (8) Use safer solvents and reaction conditions. (9) Increase energy efficiency.

(10) Design chemicals and products to degrade after use. (11) Analyze in real time to prevent pollution. (12) Minimize the potential for accidents. The term ‘safe’ in these principles refers to materials or methods less toxic for both organisms and environment, not accumulating in organisms or environment and safe to handle. Traditional nanoparticles are made of non-renewable and non-biodegradable raw materials, such as polystyrene (Menshikova *et al.*, 2005). Additionally, preparation of metallic nanoparticles often need harsh conditions and solvents. The synthesis of these traditional particles, as well as bioconjugation of the binding molecules, require variety of chemicals and solvents, and specific, often harsh, conditions and extensive purification (Chen *et al.*, 2007; Huhtinen *et al.*, 2005; Sharma *et al.*, 2008; Ye *et al.*, 2005). These multiple manufacturing steps consume energy and result in non-renewable, non-biodegrading particles. In contrast, biotechnological, and especially microbial material production inherently complies with many of the principles of green chemistry (Chang and Keasling, 2006).

All in all, identical and stably functionalized particles are often difficult and expensive to produce. Economy and straightforward production are particularly important in applications that need large amounts of homogeneous functionalized particles, such as commercial applications employing nanoparticles. Sustainable ways of producing nanoparticles, and material safety regarding both organisms and environment are aspects that need to be considered for future applications. Consequently, efforts have been devoted to developing new nanomaterials for particle synthesis and alternative methods of such synthesis and functionalization (Douglas and Young, 1998; Flenniken *et al.*, 2003; Sengupta *et al.*, 2008; von Maltzahn *et al.*, 2008).

A novel nanoscale group of structures that is gaining increasing interest is composed of biological or biologically produced materials, and these developments have been reviewed by several researchers (Katz and Willner, 2004; Sarikaya *et al.*, 2003; Uchida *et al.*, 2007). For example, various virus coats have been used as nanoparticle bodies, and microbes or microbial systems have been employed to produce metallic particles.

In the present study, a microbial production procedure is established. The process produces functionalized nanoparticles using a globular protein, apoferritin, as model for the particle. These nanoparticles are ready for use in bioaffinity assays. First, literature on ferritin is examined to reveal the several advantages offered by the protein as a modern nanomaterial, and to describe some potential applications thereof developed in recent years.

2 Ferritin

Ferritin is an iron-storing, well-conserved protein present in humans, animals, plants, and prokaryotes. Ferritin consists of 24 subunits that form a globular protein. Ferritin protein without loaded iron is termed apoferritin. Plant and prokaryote ferritins are homopolymers whereas vertebrate ferritins contain two types of subunits, heavy (~21 kDa) and light (~19 kDa) chains, as has been extensively reviewed (see, for example, Andrews *et al.* (1992)). The proportions of ferritin subunits in mammalian ferritins are tissue-dependent (Arosio *et al.*, 1978).

2.1 Ferritin structure

The structures of several ferritins have been revealed by crystallographic studies. These include structures from horse, mouse, human, *Escherichia coli,* and other microbes (Banyard *et al.*, 1978; Ford *et al.*, 1984; Hempstead *et al.*, 1997; Rice *et al.*, 1983; Stillman *et al.*, 2001; Trikha *et al.*, 1995; Wang *et al.*, 2006; Yariv *et al.*, 1981). Figure 1 shows as an example a crystallographic image of quaternary structure of ferritin consisting of human heavy chains.

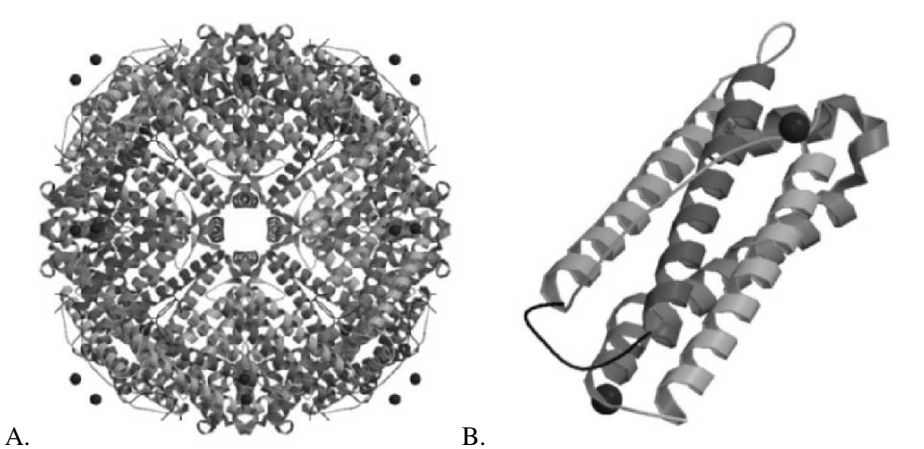

Figure 1. X-ray crystallographic structure of human ferritin. (A.) 24-meric ferritin consisting of human ferritin heavy chains and (B.) single heavy chain subunit. (PDB id: 2fha, figure adapted from Hempstead *et al.* (1997)).

The quaternary structure of ferritin (*i.e.*, the globular protein shell) is well-conserved. The 24 ferritin subunits fold to form a globular protein coat approximately 12 nm in outside diameter, and the internal cavity diameter is about 8 nm (Figure 2A). The N-terminal ends of subunits are located on the ferritin surface and the C-terminal ends point toward the inner cavity (Figure 2B). Also the ferritin subunits of several organisms studied to date have similar conformations even though amino acid sequence similarity can be low (*e.g.*, even as low as 20% for bacterial and mammalian heavy chains) (Andrews *et al.*, 1991). For example, human heavy and light chain polypeptides share a sequence similarity of only 55% but they naturally co-assemble to form heteropolymeric ferritin (Arosio *et al.*, 1978; Lawson *et al.*, 1991). Even hybrid ferritins have been generated (*e.g.,* ferritin with a mixture of human and mouse subunits) (Rucker *et al.*, 1997).

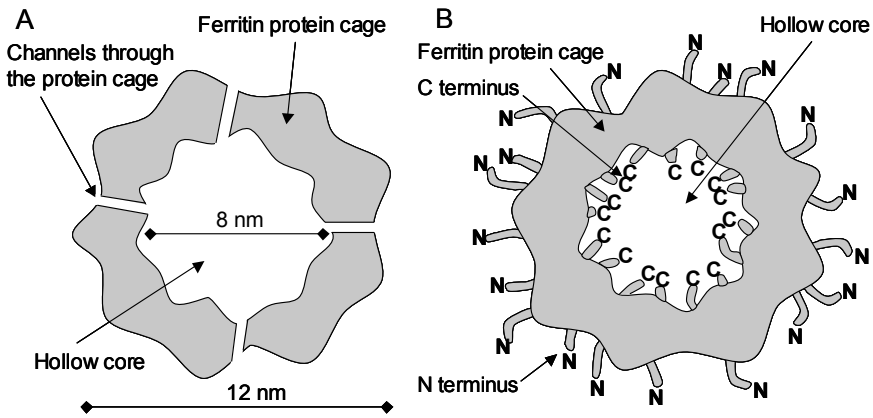

Figure 2. Schematic representations of ferritin (cross section). A. Ferritin is globular, hollow protein with outer and inner diameters of 12 nm and 8 nm, respectively. The protein coat is perforated by several small channels. B. Ferritin consists of 24 subunits, the amino-termini (denoted with N) of which protrude from the protein outer surface. The carboxy-termini (denoted with C) are located in the inner cavity of the protein.

The subunits fold to form a bundle of four α-helixes (A-D, named in order from the amino terminus), with one short α-helix (E) in the carboxy-terminal end lying at a 60° angle with respect to the four-helix bundle (Figure 3A) . A long, mainly non-structural loop connects α-helixes B and C and the turns between the helical portions and both polypeptide ends are non-structural (Figure 3A). The interior of the four-helix bundle is hydrophobic, except for the central region, which has specific functions in both heavy and light subunits (Figure 3B). The four-helix bundle is stabilized by salt bridges, hydrogen bonds, and hydrophobic interactions between α-helices and non-structural portions, especially the N-terminus. The α-helix E probably further stabilizes subunits by hydrophobic contacts and hydrogen bonds with α-helices (B, C and D) (Banyard *et al.*, 1978; Hempstead *et al.*, 1997; Jappelli *et al.*, 1992; Lawson *et al.*, 1991).

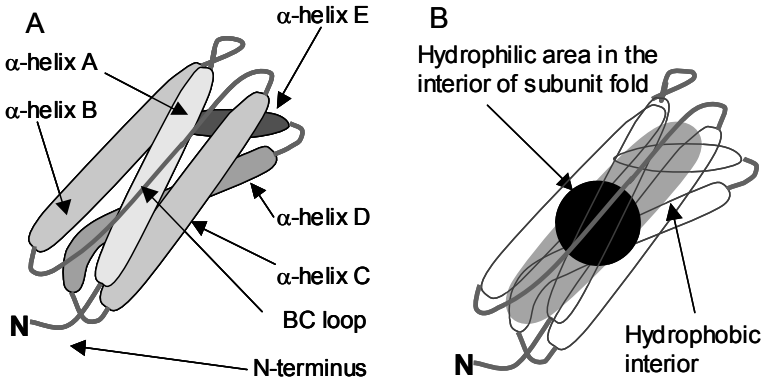

Figure 3. Schematic representations of ferritin subunit. A. The subunit consists of bundle of four long, roughly parallel α-helical portions (A-D) and one shorter α-helix (E) at an 60° angle to the bundle (α-helices are symbolized by the "sticks"). The helices are joined by non-helical portions, the longest of these being between helices B and C. B. The interior of the four-helix bundle is mainly hydrophobic (light grey area) with hydrophilic area in the centre (dark circle) in which certain important functions of ferritin reside.

Ferritin subunits assemble further into a 24-meric structure that is characterized by two-, three-, and four-fold symmetry axes (Figure 4). The interfaces between subunits are stabilized by both hydrophobic and hydrophilic forces, with the hydrophilic forces often being mediated by water molecules (Hempstead *et al.*, 1997). It has been shown that in addition to α-helices, many non-helical regions such as the N-terminus and loop regions (*e.g.,* the long loop between the B and C α-helices, and some shorter inter-helix loops) function in maintenance of structure of the 24-meric protein (Hempstead *et al.*, 1997; Jappelli and Cesareni, 1996; Jappelli *et al.*, 1992). Each two-fold axis consists of subunit dimers, in which the subunits settle in an anti-parallel direction (Figure 4A). These dyad structures are the first and probably most stable intermediates in the folding process that eventually forms the ferritin quaternary structure. However, there is no consensus regarding the intermediates that follow before the complete protein structure is obtained (Ford *et al.*, 1984; Gerl *et al.*, 1988; Santambrogio *et al.*, 1997; Stefanini *et al.*, 1987). The dimer is firmly held together by hydrophobic forces in the middle and hydrophilic forces at the ends of the helices (both helical-and non-helical portions). Importantly, also the long loops between the B and C α-helices stabilize the dimer by forming a short pleated sheet structure and through van der Waals forces. Each three-fold axis consists of three ferritin subunits that form well-conserved hydrophilic channels through the protein shell into the cavity (eight channels per ferritin molecule) (Figure 4B). In addition to acting as connections between helices of the participating subunits, the N-terminal end of the subunits stabilize the three-fold axis. Only relatively late regarding the research on ferritin it has been discovered that this three-fold channel may actually be a gated pore, which opens in certain physiological conditions (Liu *et al.*, 2003). The role for this gate is presumably releasing the iron for cellular use, the process, which has long been unresolved (Liu *et al.*, 2003; Takagi *et al.*, 1998). Each four-fold axis is formed by four subunits, usually via hydrophobic interactions between the E α-helices of the subunits, thereby creating a small hydrophobic channel within the axis (Figure 4C). The channels (six per ferritin molecule) are rich in leucine residues (Banyard *et al.*, 1978; Hempstead *et al.*, 1997; Luzzago and Cesareni, 1989). There is some evidence that the carboxy-terminal E α-helices are not essential for correct protein folding, and they can, under certain conditions, even be flipped to the outside of the ferritin core. Although C-terminal mutations do not necessarily affect the folding process of ferritin *in vivo*, such mutations have marked effects on ferritin stability and prevent protein folding *in vitro* (Jappelli *et al.*, 1992; Luzzago and Cesareni, 1989).

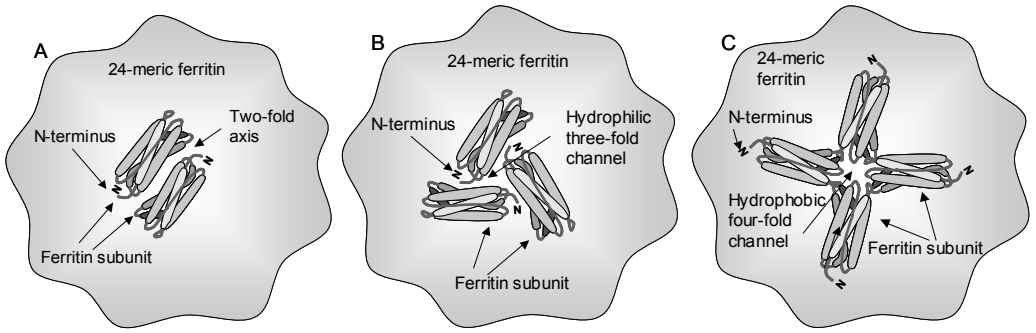

Figure 4. Schematic representations of two-, three-, and four- fold axes of ferritin 24-meric structure. A. The two-fold axis is formed of two subunits settled in antiparallel direction. These are first and probably most stable intermediate structures of ferritin. B. Three-fold axis consists of three subunits that form a hydrophilic channel perforating ferritin cage. C. Four-fold axis is mainly formed by α-helices E of four subunits. They form a leucine-rich hydrophobic channel through the protein cage.

The non-conserved amino acid residues (*e.g.,* those that differ when light and heavy chains are compared, or chains are compared between species) are mostly located inside the folded subunits and on both inner and outer protein surfaces (Hempstead *et al.*, 1997; Santambrogio *et al.*, 1992). Highly conserved amino acids are concentrated in the interfaces of the subunits and in important intra- and inter-subunit salt bridges (both in helical and non-structural portions), thereby confirming the overall conservation of protein structure. Channels on both the three- and four-fold axis interfaces contain many conserved amino acid residues whereas the two-fold interface consist principally of amino acid residues showing similar chemico-physical features (Hempstead *et al.*, 1997; Levi *et al.*, 1988).

2.2 Ferritin properties

The well-conserved structure of ferritin is responsible for several characteristics that make the protein an intriguing material for biotechnology applications. Special features of ferritin are stability and an ability to bind several metal ions. Biological functions of ferritin inside living organisms are mainly related to iron homeostasis. Ferritin mineralizes iron inside the hollow core, thereby keeping iron readily available but in a non-toxic (*i.e.,* non-reduced) form (Cozzi *et al.*, 1990). In addition to iron storage, ferritin has other biological functions, but these functions have not been studied extensively. The ferritin H-chain has been reported to have an anti-oxidant function in some patho-physiological conditions (*e.g.*, ischemia, inflammation, exposure to xenobiotics) and ferritin has been proposed to regulate protein synthesis and cell proliferation (Broxmeyer *et al.*, 1986).

The relationships between ferritin structure and functionality have been (and are still being) studied using chemical modifications and various mutant proteins. Same methods have long been used for analyzing ferritin properties. Iron loading mechanisms have mainly been revealed by spectroscopic detection of particular iron intermediates or the final iron core (Levi *et al.*, 1988). Spectroscopic methods are still used in contemporary kinetic and mechanistic studies (Bou-Abdallah *et al.*, 2004). Transmission electron microscopy (TEM) has often been

employed in work with ferritin (Wade *et al.*, 1991). Ferritin stability has been assessed mainly through the use of electrophoresis-based and spectroscopic (*e.g.,* circular dichroism) methods (Ingrassia *et al.*, 2006; Santambrogio *et al.*, 1992), and to some extent with X-ray crystallography (Butts *et al.*, 2008).

2.2.1 Iron storage function

Ferritin can take in up to 4,500 Fe^{3+} ions as a mineral core. The iron intake process includes Fe^{2+} ion movement, oxidation, and storage as a hydrated iron oxide mineral, the so-called ferrihydrite, that contains iron oxide and water molecules ($X\ Fe_2O_3 \cdot Y\ H_2O$) (Harrison *et al.*, 1967; Towe and Bradley, 1967). The iron core of ferritin is electron-dense, and can thus be visualized using TEM, without additional staining. Natural ferritin iron cores often contain traces of phosphate adsorbed on their surfaces, and bacterial ferritins (for example) have higher phosphate contents than mammalian ferritin, thereby lowering the degree of crystallinity of the iron cores (Mann *et al.*, 1986; Rohrer *et al.*, 1990; Treffry and Harrison, 1978).

The details of the mechanism by which iron is mineralized inside ferritin are still unclear; several possible mechanisms have been proposed and a number of mineralization intermediates have been observed. Most studies have been performed *in vitro* and the conclusions may not necessarily apply *in vivo*. For example, it has been shown that a homopolymer of ferritin light chain is able to load iron *in vitro* but not under physiological conditions *in vivo* (Arosio *et al.*, 1977; Santambrogio *et al.*, 1996). However, three different, and likely concurrently operating iron loading mechanisms have been identified and widely accepted. They are summarized in Figures 5 and 6.

First, Fe^{2+} ions probably enter ferritin through the channels of the three-fold axes that are known to have carboxyl group-based metal ion binding sites (Lawson *et al.*, 1991; Macara *et al.*, 1973; Stefanini *et al.*, 1989; Treffry *et al.*, 1993; Wardeska *et al.*, 1986). In addition, there is one possible path through each heavy chain, which is not available in light chains (Lawson *et al.*, 1991).

The presumably main iron mineralization mechanism is presented in Figure 5. Based on several studies using homopolymeric ferritins, the heavy and light chains were shown to have partially complementary roles. It is therefore to be expected that the two subunits will co-operate in the main process of iron storage in ferritin (Levi *et al.*, 1994b). Ferritin heavy chains have a distinct dinuclear center with a catalytic (ferroxidase) function, which rapidly oxidizes Fe^{2+} ions to Fe^{3+} using O_2 or some other electron acceptor, producing H_2O_2 and four H^+ ions as by-products (Kadir *et al.*, 1991; Lawson *et al.*, 1989; Watt *et al.*, 1988; Xu and Chasteen, 1991; Yang and Chasteen, 1999). The ferroxidase site is located close to the three-fold channel, in a hydrophilic region in the center of an otherwise hydrophobic α-helix bundle (Figure 3B), and consists of six amino acid residues (five Glu and one His) that are conserved in almost all known ferritins except the light chain ferritins (Santambrogio *et al.*, 1996; Trikha *et al.*, 1995) (several sequences have been summarized in the review by Andrews *et al.* (1992). These amino acid residues form ligands for two Fe^{2+} ions, hence the designation dinuclear center (Sun *et al.*, 1993). Further processing of Fe^{3+} includes movement into the hollow cavity and formation of

the mineral core. Ion movement from the ferroxidase site probably occurs with the aid of an electrostatic potential that directs Fe^{3+} cations to the interior of ferritin (Douglas and Ripoll, 1998). Light chain subunits are mainly responsible for mineral core formation, the so-called nucleation, probably via six negatively charged Glu residues located on the interior surface of ferritin (Levi *et al.*, 1994b; Santambrogio *et al.*, 1996). There is also an indication that an electrostatic potential may enhance Fe^{3+} ion flux into nucleation sites, because the negatively charged Glu patch is partially surrounded by positive charges (Douglas and Ripoll, 1998). Ferritin heavy chains contain some of these Glu residues, which have been suggested to be involved as nucleation centers; however, they are not necessary for iron mineralization (Bou-Abdallah *et al.*, 2004; Lawson *et al.*, 1991). Overall, these distinct carboxylate groups in both heavy and light chains are vital for efficient iron mineralization.

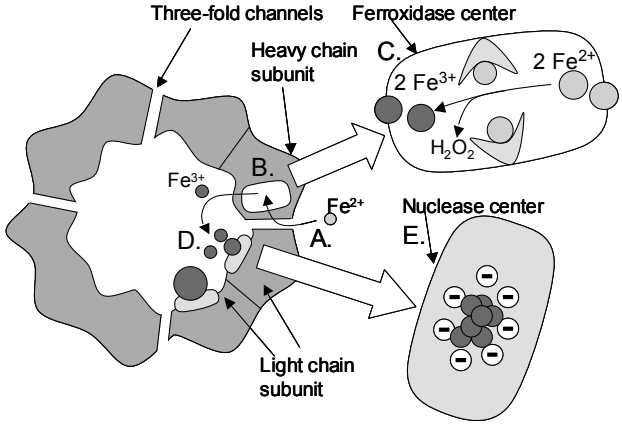

Figure 5. Main process in ferritin iron mineralization that probably includes co-operation of heavy and light chains. Fe^{2+} enters ferritin via the three-fold channel (A), from which it is driven to dinuclear ferroxidase centre inside the ferritin heavy chain (B). Fe^{2+} is oxidized to Fe^{3+} in ferroxidase centre (magnified in C). Fe^{3+} ions enter ferritin cavity and are driven to the nuclease centre of the light chain (D) (on the inner surface of the protein cage). The mineralization of Fe^{3+} begins in the negatively charged nuclease centre (magnified in E).

As the ferroxidase-based mechanism proceeds, another Fe^{2+} oxidation reaction takes place, in which the H_2O_2 produced in the ferroxidase reaction oxidizes more iron, and H_2O_2 is detoxified (Figure 6A) (Zhao *et al.*, 2003). In addition, a third reaction relevant to Fe^{3+} storage occurs on the mineral surface inside ferritin; this is auto-oxidation of Fe^{2+} (Figure 6B). This reaction becomes predominant as the amount of Fe^{2+} ions increases, and when the core is already formed or when no significant ferroxidase activity is present (Levi *et al.*, 1988; Macara *et al.*, 1972; Sun *et al.*, 1993; Zhao *et al.*, 2003).

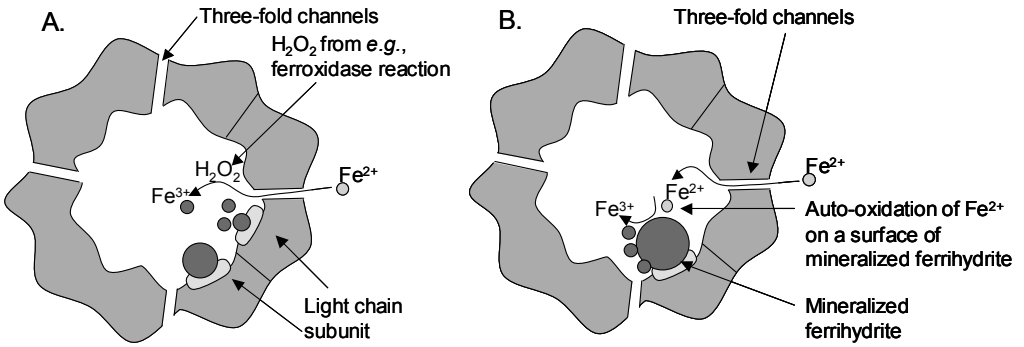

Figure 6. Two other iron mineralization processes in ferritin. A. H_2O_2 is produced during ferroxidase function of heavy chain subunits. Ferritin can partly utilize H_2O_2 to oxidize Fe^{2+} to Fe^{3+} within ferritin. Fe^{3+} is probably mineralized in nucleation centre of ferritin light chain subunit. B. Fe^{2+} can auto-oxidize to Fe^{3+} on the surface of formed mineral cores. This mechanism is predominant at high iron loadings.

Homopolymers of light and heavy chains are able to mineralize iron *in vitro* even though iron uptake efficiency is highest when heteropolymers are used (Levi *et al.*, 1994b). Homopolymers show differences in iron loading. Heavy chain homopolymers with ferroxidase activity load iron faster than light chain apoferritin. However, light chain homopolymers are able to take up iron *in vitro* at pH values above 7.0 even more efficiently than heavy chains at high iron loadings (Levi *et al.*, 1989b; Santambrogio *et al.*, 1996). In addition, larger and more defined iron cores are formed, and higher quantities of Fe^{2+} ions are tolerated, by ferritin consisting of light chains. In acidic conditions and in the presence of phosphate or citrate, light chain apoferritin is not able to load iron even *in vitro* (Levi *et al.*, 1989b; Santambrogio *et al.*, 1996). The mechanism of light chain homopolymer iron loading is probably based on iron auto-oxidation (Figure 6B), which is more efficient inside ferritin than in solution, and bulk iron precipitation is therefore efficiently inhibited (Levi *et al.*, 1994b; Santambrogio *et al.*, 1996; Wade *et al.*, 1991). The light and heavy chains have co-operative roles in complete, 24-meric, ferritin, and the ratio of heavy-to-light chains affects ferritin functionality. In general, heavy chains speed up iron incorporation (although maximum incorporation is seen at 35% heavy chain content), and light chains both confer improved stability (See below) and inhibit protein aggregation at high Fe^{2+} loads (Levi *et al.*, 1994b; Santambrogio *et al.*, 1993).

In conclusion, iron mineralization in ferritin is a robust process. Several mutations can be tolerated; these affect mainly the shape and size of the iron core. Only major structural changes, or specific changes in some amino acids of either ferroxidase or the nucleation sites, seriously inhibit ferritin iron loading (Lawson *et al.*, 1989; Levi *et al.*, 1989a; Treffry *et al.*, 1993; Wade *et al.*, 1991) Various substances, for example several cations and anions, have been reported to enhance or inhibit iron loading, but in practice the effects are minor, varying loading times by a few minutes to a few hours (Cheng and Chasteen, 1991; Cutler *et al.*, 2005; Polanams *et al.*, 2005).

2.2.2 Protein stability

Ferritin is exceptionally stable. Several experiments have shown that the 24-meric protein coat can endure temperatures up to 80°C and extremes of pH (Crichton and Bryce, 1973; Santambrogio *et al.*, 1992). Therefore, heat treatment is generally used as a purification step when isolating ferritin from various biological matrices. The full denaturation of for example, horse spleen ferritin can be accomplished by treating protein at a pH below 3, boiling in 1% (w/v) SDS, or treating protein with high urea or guanidine hydrochloride concentrations under acidic conditions (Crichton and Bryce, 1973; Listowsky *et al.*, 1972). Ferritin stability is also reflected by the fact that (at least) human ferritin subunits (both heavy and light chains) can readily refold *in vitro* after denaturation (Santambrogio *et al.*, 1993; Smith-Johannsen and Drysdale, 1969).

The causes of such impressive stability are probably the relatively high number of both inter- and intra-subunit salt bridges. In addition, tight subunit packing may have a stabilizing effect (the surface-to-volume ratio is low) (Hempstead *et al.*, 1997). The iron core inside ferritin does not affect at least to the thermal stability of ferritin (Stefanini *et al.*, 1996). In general, several amino acid changes are tolerated without changes in ferritin folding or resistance to physical stress. This is understandable, considering the large variations in ferritin primary sequences. However, mutations in regions that have conserved amino acids may have serious effects. Protein folding may be completely inhibited, or ferritin may fold to the quaternary structure but protein stability or iron loading ability may fall. Figure 7 summarizes some of the critical parts of subunit that affect ferritin functionality. Loop sequences have been deduced to be relatively sensitive to mutation, especially amino acid substitutions and deletions reflecting their participation in stabilizing the subunit dimers. Such mutations often have dramatic effects, and may completely prevent protein folding or may cause aggregation of the folded protein (Jappelli and Cesareni, 1996; Jappelli *et al.*, 1992; Levi *et al.*, 1989a; Santambrogio *et al.*, 1997). Variants that often retain folding ability but with impaired stability of the protein shell have been reported to be deletions of the N-terminus (13 amino acids) or C-terminus (22 amino acids), or to have particular changes in the channels, the two-fold interfaces, or the C-terminus. The effects on iron incorporation have often been less severe, and only major mutations totally block iron loading (Ingrassia *et al.*, 2006; Levi *et al.*, 1988; Levi *et al.*, 1989a; Santambrogio *et al.*, 1992; Wade *et al.*, 1991; Yoshizawa *et al.*, 2007). Amino acid insertions have been described to be relatively well-tolerated for example in loop sections, the N-terminus and, to some extent, the C-terminus (Levi *et al.*, 1989a; Yoshizawa *et al.*, 2007). An N-terminal, α-helical polypeptide (29 amino acid residues) extension of ferritin may even assist in ferritin stability. Improved thermal stability of the mutant at high protein concentrations has been shown (Kim *et al.*, 2001).

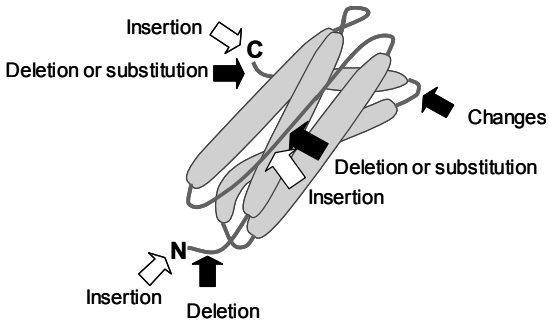

Figure 7. Areas of ferritin subunit that are affected by certain mutations in amino acid sequence. Amino acid deeletions and certain substitutions (black arrows) cause impaired ferritin function. Most vulnerable areas are usually those having inter- or intra-chain interactions in ferritin assembly. Usually the insertions in these areas are tolerated relatively well (denoted with white arrows)

The light chains of ferritin are more stable than the heavy chains. The refolding kinetics of the two ferritin chains are similar although heavy chain denaturation is faster (Santambrogio *et al.*, 1993). The enhanced stability of the ferritin light chain is conferred mainly by a salt bridge, which resides in the hydrophilic patch inside the α-helix bundle (Figure 3B). This salt bridge is enabled by two amino acid substitutions of the heavy chain ferroxidase center (Glu to Lys and Glu to Gly), after which the salt bridge is formed between Lys and one additional Glu of the ferrioxidase center (Figure 3) (Hempstead *et al.*, 1997; Lawson *et al.*, 1991; Santambrogio *et al.*, 1992). Additionally, the better stability of the light chain extends to the whole protein assembly. When light chains are mixed with heavy chains the stability of the 24-meric protein is increased as the light chain proportion rises (Santambrogio *et al.*, 1993). With this effect even mutated subunits may be tolerated if "diluted" with pristine subunits within the ferritin assembly (Santambrogio *et al.*, 1997).

2.2.3 Metal-binding ability

Early studies showed that (apo)ferritin had binding sites for some divalent metal cations other than iron. Metal binding abilities were identified by inhibition of (apo)ferritin iron loading using certain divalent cations and these findings have been confirmed also in X-ray crystallography studies (Lawson *et al.*, 1991; Macara *et al.*, 1973; Niederer, 1970; Rice *et al.*, 1983). At least Be^{2+}, Cd^{2+}, Ca^{2+}, Cr^{3+}, Cu^{2+}, Mn^{2+}, Tb^{3+}, UO_2^{2+}, VO^{2+}, and Zn^{2+} ions are bound by the (apo)ferritin interior surface (*e.g.*, the three-fold channels or the cavity) and Cd^{2+} is additionally bound on the ferritin surface. The binding sites for different cations may vary and some ions have several binding sites with different binding affinities (Grady *et al.*, 2000; Hoare *et al.*, 1975; Macara *et al.*, 1973; Pead *et al.*, 1995; Price and Joshi, 1983; Treffry and Harrison, 1984; Wardeska *et al.*, 1986; Wauters *et al.*, 1978). For example, Tb^{3+} appears to have a binding site in the channel of the three-fold axis whereas Zn^{2+} ion may bind to the ferroxidase site (Treffry *et al.*, 1993). The number of bound metal ions is typically 30-40 per apoferritin, depending on the pH, indicating

that most metal binding sites consist of amino acid residues with carboxyl groups (Chasteen and Theil, 1982; Treffry and Harrison, 1980).

In addition, native ferritin, (*i.e.,* ferritin with an iron core including some phosphate) is able to bind several cations (*e.g.,* Be^{2+}, Cd^{2+}, Zn^{2+}) to an extent greater than shown by apoferritin or even by ferritin without phosphate. This binding is probably aided by phosphate on the surface of the iron core. This indicates that ferritin may have a physiological role in detoxification of metal cations other than iron, a feature that may be deleterious for an organism in some cases (Atkinson *et al.*, 2005; Pead *et al.*, 1995; Price and Joshi, 1982; Price and Joshi, 1983).

2.3 Ferritin-like proteins

Ferritin-like proteins, Flps, include microbial proteins that generally function in protecting bacterial DNA and bacterial cells against oxidative damage (H_2O_2 or $O_2\cdot$). These proteins are termed Dps proteins (**D**NA-binding **p**roteins during **s**tationary phase) and Dpr (**D**ps-like **p**eroxide-**r**esistance) proteins, with reference to their principal functional modes. Flps have several characteristics resembling those of ferritin, but also show distinctive features, and are hence termed ferritin-like proteins. Flps from several microbes have been studied; the work has been reviewed by Smith (2004) together with data on the actual ferritins of the same microbes.

Ferritin-like proteins consist of 12 subunits (each about 18 kDa) that fold in a four-helix bundle as do the subunits of 24-meric ferritins, but the E α-helix does not exist in Flps (Ceci *et al.*, 2003; Ilari *et al.*, 2000). The 12 subunits also form a globular, hollow, protein but the outer and inner diameters are 9 nm and 4.5 nm, respectively. The quaternary structure features a 2/3 assembly (*i.e.,* Flps show only two- and three-fold symmetry axes). The structures of at least some Flps resemble that of ferritins with respect to stability because heat-treatment (65°C) has been successfully used as a purification step for certain Flps (Allen *et al.*, 2002; Kramer *et al.*, 2005). Those Flps that are able to store iron have a ferroxidase site, which, however, is located in an area (at the interface of two subunits) distinct from that of ferritin, and the site contains different amino acid residues than are found in actual ferritins (Su *et al.*, 2005). The iron storage mechanisms of Flps and ferritins may thus differ somewhat; Flps store iron faster in the presence of H_2O_2 whereas the main mechanism of iron storage used by ferritins employs O_2. Because Flps are smaller than ferritins, a Flp takes up only approximately 500 iron ions (4,500 for ferritin) (Bozzi *et al.*, 1997). Because of structural and functional similarities with ferritins, Flps have also been used in modern biotechnological applications developed with actual ferritins.

3 Ferritin and recombinant gene technology

Recombinant DNA technology has been used primarily for basic research on ferritin. However, this approach has also paved the way for the use of ferritin in biotechnology because microbial culture enables efficient, upscalable production of the desired protein.

3.1 Recombinant ferritin production and purification

Before the advent of recombinant DNA technology, ferritins were isolated from various tissues and organisms. Protein overexpression in fast-growing microbial cells has facilitated the study of ferritins of small organisms (*e.g.,* various prokaryotes) from which the isolation of large amounts of ferritin is difficult. *E. coli* permits the use of efficient heterologous protein expression systems and these have been applied to clone and express human ferritin chains in high yields.

Human heavy and light chain ferritin subunits were first cloned into *E. coli* cells for protein overexpression in the late 1980s, and the homopolymers were determined to have characteristics generally corresponding to features of native human ferritin (*i.e,*. formation of 24-meric protein, thermostability, and iron loading) (Levi *et al.*, 1987; Levi *et al.*, 1989b; Santambrogio *et al.*, 1993). Recombinant technology has enabled the study of ferritin homopolymers consisting of human light or heavy chains, and ferritins from other species; and since then recombinant ferritins have been used to study ferritin characteristics (as outlined above in section 2.2).

Apart from microbially-produced homopolymers, both ferritin chains have been simultaneously expressed in a bicistronic system and a dual vector system not only in *E. coli* but also in yeast, *Saccharomyces cerevisiae* (Grace *et al.*, 2000; Kim *et al.*, 2003; Rucker *et al.*, 1997). The subunits produced in *E. coli* have formed heteropolymeric ferritins of various subunit ratios; the polymers could be separated chromatographically. However, there is some controversy on whether subunit ratios vary or are relatively constant (Grace *et al.*, 2000; Rucker *et al.*, 1997). *In vitro* studies have shown that the ratios of heavy and light chains in heteropolymeric ferritins can be controlled by variation in initial subunit concentrations, so that different features of heavy and light chains can be emphasized in a heteropolymer if desired (Santambrogio *et al.*, 1993).

Recombinant, soluble ferritin is typically purified using a protocols developed for purifying ferritin from tissues (Arosio *et al.*, 1978; Crichton *et al.*, 1973). The traditional purification scheme includes heat treatment (approximately 70°C), ammonium sulfate precipitation, and both size-exclusion and anion exchange chromatography, or ultracentrifugation instead of the ion exchange chromatography. Usually at least two or three of these steps are still employed (Levi *et al.*, 1987; Swift *et al.*, 2006; Uchida *et al.*, 2008). However, alternative purification mechanisms (affinity purification, sonication-based purification combined with gel filtration, or a combination of heat treatment with high molecular weight-polyethylene glycol precipitation) have been reported (Ahn *et al.*, 2005; Huh and Kim, 2003; Luzzago and Cesareni, 1989; von Darl *et al.*, 1994).

The yields of purified recombinant human ferritins from bacterial batch cultivation are in the ranges 10-15 mg/l and 2-5 mg/l for heavy and light chains, respectively. Recently, a yield of 100 mg/l for the heavy chain has been reported (Santambrogio *et al.*, 1993; Uchida *et al.*, 2006). The higher yields of human heavy chain subunits may be related to the higher solubility of ferritin heavy chains in *E. coli* cells, and also because human ferritin light chain subunits are produced largely as insoluble inclusion bodies (Kim *et al.*, 2001). The better solubility of heavy chains has been proposed to reflect expression of a binding site for a particular chaperone (Ahn *et al.*, 2005). Ferritin light chains have been recovered from inclusion bodies by denaturing the inclusion bodies at pH 12, and then quickly refolding the light chains by shifting to pH 8. This straightforward process indicates that human light chain ferritins have formed inclusion bodies with relatively loose (non-covalent) interactions (Kim *et al.*, 2001). However, this may not be the case for certain other ferritins, for which refolding from inclusion bodies has been unsuccessful, at least under the conditions tested (Levi *et al.*, 1994a; Van Wuytswinkel *et al.*, 1995; von Darl *et al.*, 1994).

Recombinant ferritin production produces reasonably large amounts of ferritin for various applications (Hoppler *et al.*, 2008; Trikha *et al.*, 1995; Trikha *et al.*, 1994; Yamashita *et al.*, 2006). However, because the primary sequences of different ferritins vary quite significantly, efficient microbial expression of a particular ferritin may sometimes require optimization (Rucker *et al.*, 1997; Van Wuytswinkel *et al.*, 1995; von Darl *et al.*, 1994). To date, the use of recombinant ferritins has been minor in modern applications and commercial ferritins (usually isolated from horse) have been used instead. Flps used in different applications are most often recombinant.

3.2 Genetic modifications

Genetic modification has been used to examine ferritin structure, function, and characteristics, for many years. The first mutation analyses were performed when the first recombinant ferritins were produced. The ferroxidase center in heavy chains, the putative nucleation sites of heavy and light chains, and a salt bridge contributing to L-chain stability, have been identified by site-directed substitutions of amino acid residues with residues of opposite chemico-physical features. For example, the functions of heavy and light chain ferritins have been interchanged in such work (Levi *et al.*, 1994b), and deletions have been frequently used to map regions involved in ferritin folding or essential to native protein function (Levi *et al.*, 1994a; Santambrogio *et al.*, 1992). One of the first genetic fusions involving ferritin was the carboxy-terminal fusion of the ferritin heavy chain to the α peptide of β-galactosidase; the system was exploited as a reporter in the study of ferritin folding (Luzzago and Cesareni, 1989). More recently, mutations in the ferritin light chain gene have been found to be related to a neurodegenerative disorder; a phenomenon subsequently reviewed (Levi *et al.*, 2005). This has encouraged ferritin researchers to re-focus on mutation analysis, and specifically on effects of mutations on ferritin functions in eukaryotic cells (Ingrassia *et al.*, 2006; Vidal *et al.*, 2008).

The terminal ends of ferritin subunits that point out from the protein surface, or towards the relatively spacious inner cavity (Figure 2B), provide interesting sites for protein fusions. Real

biotechnological applications of genetically engineered ferritins emerged only in early 2000s, even though first amino or carboxy-terminal fusions to a ferritin subunits, associated with additional functionalities, were reported in the early 1990s (Sidoli *et al.*, 1993; von Darl *et al.*, 1994). For example, the amino terminal fusion partner, maltose-binding protein, had been used to purify ferritin by affinity chromatography, and the protein "tag" was removed after purification (See Figure 8A). The maltose-binding protein consists of 371 amino acid residues, demonstrating the capacity of a ferritin subunits to form a globular structure after fusion to a protein twice the size of the subunit itself (approximately 180 amino acids) (von Darl *et al.*, 1994). Recently, N-terminal fusions have imparted totally new properties to ferritin proteins. These applications include peptides with selective binding activities for certain metals (GEPIs; Genetically Engineered Peptides for Inorganics) and peptides targeting desired tissues or other molecules (Hayashi *et al.*, 2006; Sano *et al.*, 2005; Uchida *et al.*, 2006; Yamashita *et al.*, 2006).

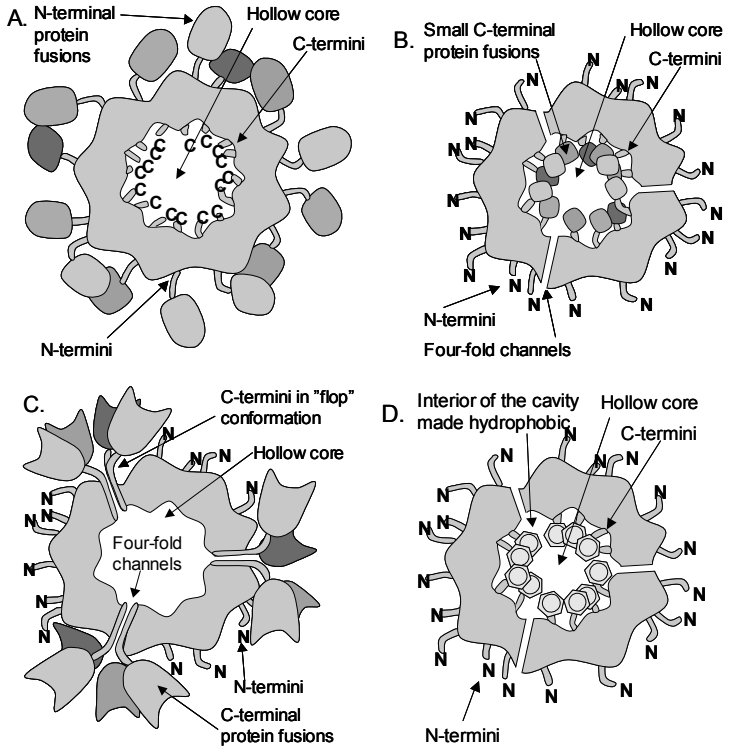

Figure 8. Sites for mutations adding new functionalities to ferritin. A. N-terminal insertions are well-tolerated, and they provide sites for displaying desired molecules on the surface of ferritin. B. Small insertions, such as peptides in C-terminal ends can also be tolerated. These can provide new features to use ferritin as nanocontainer. C. Large insertions in C-terminus may result in "flop" conformation, in which C-termini with inserted proteins/peptides point outside from the cavity, even though the stability of the ferritin cage is compromised. D. The changes in the chemico-physical features of ferritin cavity surface may alter ferritin specificity for different metals and other substances.

The inner cavity of ferritin is size-constrained, and, as has been shown by Luggazzo and Cesareni (1989), two or three 90-amino acid peptides can fit into the cavity. However, if packing becomes excessive, the C-terminal ends of ferritin monomers can switch to become directed to the outside of the ferritin, to yield the so-called "flop" conformation (Figure 8C). Under such circumstances protein coat integrity is compromised leading to loss of protein stability and inability to load iron inside the protein (Jappelli *et al.*, 1992; Levi *et al.*, 1989a; Luzzago and Cesareni, 1989). Some useful carboxy-terminal fusions of ferritin with other proteins have been reported. The "flop" conformation of the ferritin C-terminus has been utilized to display certain allergens and antigens on the ferritin surface (Figure 8C) (Choi *et al.*, 2005; Sidoli *et al.*, 1993). Another intriguing experiment has combined a GEPI with the C-terminal end of the ferritin subunit, resulting in a ferritin that generates silver particles inside the cavity (Figure 8B) (Kramer *et al.*, 2004). So far, at least two research groups have reported changes in the ferritin cavity surface using genetic engineering, with the intention of loading alternative, non-iron materials inside ferritin (Figure 8D) (Abe *et al.*, 2008; Butts *et al.*, 2008; Swift *et al.*, 2006).

4 Ferritin as a nanocontainer

4.1 Hybrid materials: proteins combined with metals

Metal or semiconducting nanoparticles conjugated to biomolecules (proteins or nucleic acids) and artificial particulate metalloproteins have several useful functions and properties (for a review, see Katz and Willner (2004). These hybrid materials are becoming more extensively studied and the focus of the work is shifting from basic research to applications, because hybrid materials have potential in various electronic, optical, and catalytic applications. Several synthesis methods are available for preparation of nanoscale metal and semiconductor particles, which often require surface-capping systems to prevent particles from aggregating into a bulk material and to control particle size. Some of these preparation methods have been reviewed by Masala and Seshadri (2004). Metallic particles combined with specific proteins or other biomolecules as capping agents are receiving increasing attention. For example, proteins enhance particle water solubility, minimize particle aggregation and bring specific recognition or catalytic features to the metallic particles. Preparation mechanisms for these artificial metalloproteins are based on (1) covalent or non-covalent cross-linkage between the protein and metal complex, (2) accretion of metals with proteins (*e.g.,* using GEPIs), (3) use of proteins (such as ferritin) naturally mineralizing metals, or (4) encapsulation of metals in protein cages (such as capsids of viruses).

Certain protein cages, such as various viral capsids (Douglas and Young, 1998) devoid of nucleic acids and heat-shock proteins (Flenniken *et al.*, 2003), provide size- and shape-constrained templates for the synthesis of metallic nanoparticles (for a review see Uchida *et al.* (2007)). Metallic particles based on biological templates or protein cages sometimes enable particle production under significantly milder conditions than feature in conventional inorganic reactions (Ensign *et al.*, 2004; Iwahori *et al.*, 2005; Klem *et al.*, 2005; Lee *et al.*, 2002; Okuda *et al.*, 2003). On the other hand, protein cages should preferably resist relatively harsh conditions (*e.g.*, wide pH range and high temperature) when used in the generation of particular metallic compounds (Meldrum *et al.*, 1992; Wiedenheft *et al.*, 2005). The minimal criteria when a protein is to be used as a template are as follows (Figure 9): (1) A cagelike structure that can spatially separate metal particles from the outer solvent is required. (2) Chemically or electrostatically distinct exterior and interior surfaces are needed to allow appropriate ions to concentrate inside the protein. (3) The desired molecules or ions must be able to migrate inside the protein cage (Douglas and Young, 1998).

The protein core of ferritin fulfills all the criteria mentioned above (*i.e.,* ferritin has three- and four-fold channels through the protein and a negatively charged interior surface with an electrostatic potential directing cations from outside to the cavity) in addition to good physical stability, and, hence, ferritin has been successfully used in studies preparing protein-templated nanoparticles. Also, various compounds that do not form nanoparticles have been loaded inside the ferritin cage, thus using the protein as a nanocontainer.

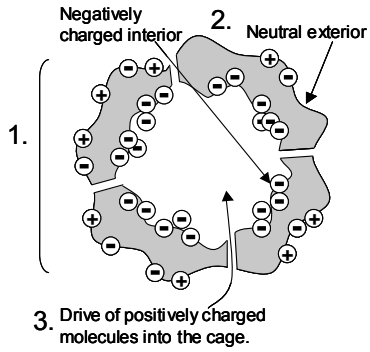

Figure 9. Minimal criteria for a protein to act as a template for creating metallic nanoparticles. Cations are here as an example for the starting material. (1) A cage-like structure for size-constrained particle synthesis, (2) Distinct exterior and interior surfaces, and (3) a route for desired ions to move inside the cage.

4.2 Ferritin as a nanocontainer (metals and other compounds)

Nanoparticles of several metal compounds, and different approaches for generating such nanoparticles inside apoferritin or ferritin cavities, have been described. Additionally other, relatively large compounds such as drugs have also been loaded in ferritin. Basically, four approaches are taken (Figure 10). Most methods are based simply on diffusion of various ions and compounds into apoferritin under specific conditions (Figure 10A) (Douglas and Stark, 2000; Hosein *et al.*, 2004; Meldrum *et al.*, 1995; Meldrum *et al.*, 1991; Okuda *et al.*, 2003). The cores of both natural and non-natural ferritins are catalytic under certain conditions, or can undergo *in situ* reactions (Nikandrov *et al.*, 1997; Ueno *et al.*, 2004), and new materials have been created utilizing these features (Figure 10B). Ferritins have been used in photochemical reactions, in which ferritin with associated iron oxide catalyzed reduction of metals (Cr^{6+}, Cu^{2+}) in the presence of UV/visible light to produce colored metallic particles (Ensign *et al.*, 2004; Kim *et al.*, 2002). Alternatively, various chemicals can be used to transform the preformed cores of non-natural or natural ferritins (Galvez *et al.*, 2005; Meldrum *et al.*, 1991; Ueno *et al.*, 2004). The refolding ability of apoferritin has been used to passively (in part) encapsulate various metal particles and other compounds. In these procedures, the protein cage is dissolved at extreme pH (pH 2 or pH 12) and the desired compounds are passively encapsulated within the protein cores by returning the pH to neutral (Figure 10C) (Webb *et al.*, 1994). This approach has often been exploited in recent years because it enables loading of larger molecules than can pass through the apoferritin channels. Thus, in addition to the synthesis of metallic particles inside apoferritin, other substances such as metal chelates, drugs and even ready particles can be loaded inside the ferritin protein cavity (Dominguez-Vera and Colacio, 2003; Hennequin *et al.*, 2008; Webb *et al.*, 1994). An additional novel approach uses GEPIs fused to ferritin subunits to drive the formation of desirable metal particles (Figure 10D) (Kramer *et al.*, 2004). Examples of compounds loaded or generated with the aid of apoferritin (or ferritin) and ferritin-like proteins

are presented in Table 1. The examples are organized by the loading methods utilized, as shown in Figure 10.

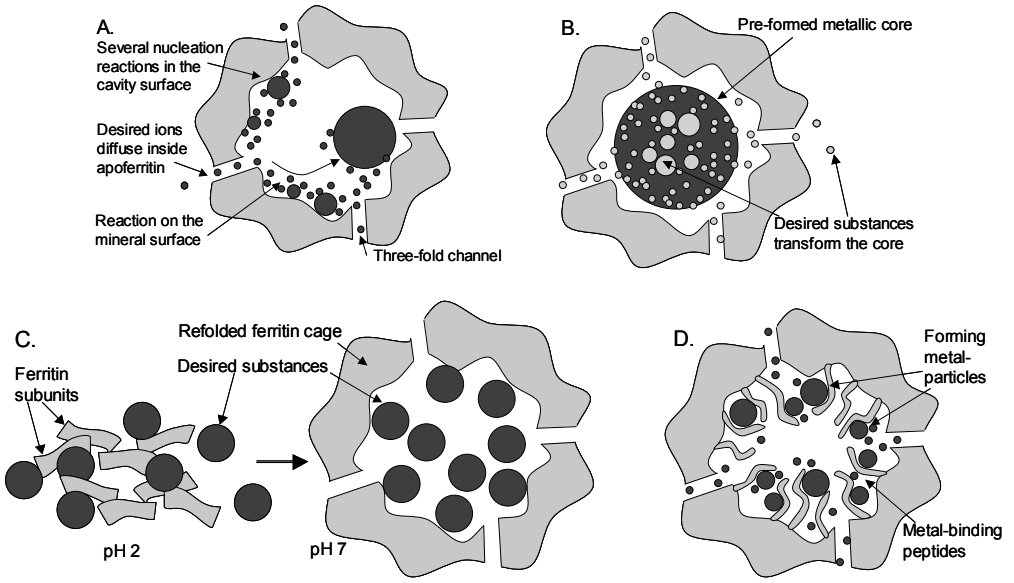

Figure 10. Ferritin-loading approaches. A. The desired ions diffuse inside apoferritin and form particles by some reaction (e.g., auto-oxidation). The reaction starts often at multiple sites on the cavity surface forming several small incipient particles that grow and finally merge. B. Ferritin or apoferritin loaded with some metal (Method in A) can be *in situ* transformed to another material. C. By denaturing (*e.g.*, pH 2) and refolding (*e.g.*, pH 7) apoferritin protein cage substances can be encapsulated inside ferritin cage. D. Using metal-binding peptides desired materials can be loaded inside apoferritin.

Table 1. Different substances loaded into apoferritin, or particles formed using ferritin or apoferritin. The materials are organized by loading method. Potential features or functionalities of the particles, as stated by the researchers, are presented, as well as source of ferritin used and reported application of the material.

Material loaded in or formed using ferritin / apoferritin	Potential particle features or functions stated in respective references	Source of ferritin	Demonstrated application / functionality	Reference
Loading methods that are based on diffusion on one or several ions.				
Cadmium sulfide (CdS) particles.	Semiconducting particles.	Horse spleen apoferritin	N/A, preliminary work.	(Wong and Mann, 1996)
	Semiconducting particles, possibly utilizable in nanoelectronics, photoluminescent.	Recombinant ferritin-like protein used.	Particles show some photoluminescence even though they are polycrystalline.	(Iwahori *et al.*, 2007)
Cadmium selenide (CdSe) particles.	Semiconducting particles possibly utilizable in nanoelectronics and photoluminescence.	Horse spleen apoferritin used.	N/A.	(Iwahori *et al.*, 2006; Yamashita *et al.*, 2004)
Carbonate particles of calcium, strontium, or barium (and calcium phosphate).	N/A.	Apoferritin from horse spleen ferritin used.	N/A, new reaction model.	(Li *et al.*, 2007)
Chromium particles.	Possibly usable in nanoelectronics.	Both horse spleen apoferritin and recombinant apoferritin used.	N/A.	(Okuda *et al.*, 2003)
Cobalt oxyhydroxide/ oxide particles.	N/A.	Horse spleen apoferritin used.	N/A (Color, olive green).	(Douglas and Stark, 2000)
	Magnetic and catalytic particles	Recombinant ferritin-like proteins used.	N/A.	(Allen *et al.*, 2003)
	Magnetic, catalytic, possibly utilizable in nanoelectronics.	Horse apoferritin used.	N/A, apoferritin loading mechanism studied.	(Kim *et al.*, 2005)

	Magnetic, catalytic, possibly utilizable in nanoelectronics.	Recombinant ferritin-like protein used.	Magnetism showed.	(Resnick *et al.*, 2006)
Co_3O_4 to Co (metallic) particles.	Magnetic and catalytic.	Recombinant ferritin-like protein used.	N/A.	(Hosein *et al.*, 2004)
Europium, iron, titanium particles (oxides).	N/A.	Commercial mammalian apoferritin used.	N/A, new type of loading method (high-oxidation state ions).	(Klem *et al.*, 2008)
Gold particles.	Catalytic.	N/A.	Single-walled carbon nanotubes were produced using the gold particles produced with ferritin.	(Takagi *et al.*, 2007)
	Surface plasmon resonant particles, catalytic properties.	Horse spleen apoferritin used.	N/A.	(Zhang *et al.*, 2007)
	Surface plasmon resonant particles.	Recombinant apoferritin used. Apoferritins were mutated to possibly optimize the loading.	Surface plasmon resonance of the particles shown.	(Butts *et al.*, 2008)
Gold sulfide particles.	Semiconducting particles, possibly utilizable in nanoelectronics.	N/A.	Apoferritin coating confers water solubility of Au_2S particles.	(Yoshizawa *et al.*, 2006)
Indium oxide particles.	Possibly utilizable in nanoelectronics.	Recombinant apoferritin used.	N/A.	(Okuda *et al.*, 2005)
Iron arsenate, phosphate, vanadate, molybdate particles.	Catalytic.	Horse spleen apoferritin used.	N/A.	(Polanams *et al.*, 2005)
Iron cobalt particles (oxide) (FeCo).	Magnetic.	Commercial apoferritin used.	Magnetism showed with ferritin.	(Klem *et al.*, 2007)

Iron oxide particles (*i.e.,* regular ferrihydrite).	Catalytic.	Commercial apoferritin and ferritin used.	Ferritin acting as photocatalyst in presence of UV/visible light.	(Kim *et al.*, 2002; Nikandrov *et al.*, 1997)
	Catalytic.	Both recombinant ferritin-like proteins and regular ferritins have been used.	Iron oxide without ferritin protein catalysed production of carbon nanotubes.	(Kramer *et al.*, 2005)
	Catalytic.	Commercial apoferritin was used.	Ferritin acting as photocatalyst in presence of visible light reducing copper.	(Ensign *et al.*, 2004)
Iron oxide particles (magnetic).	Magnetic particles. Potential as MRI contrast agent.	Horse spleen apoferritin used.	Magnetism showed.	(Bulte *et al.*, 1994a; Bulte *et al.*, 1994b; Meldrum *et al.*, 1992; Wong *et al.*, 1998)
	Magnetic.	Apoferritin from horse spleen ferritin used.	Magnetic ferritin used to label and separate certain cells.	(Zborowski *et al.*, 1996)
	Magnetic.	Recombinant ferritin-like proteins used.	Magnetism showed.	(Allen *et al.*, 2002)
	Magnetic, Potential as MRI contrast agent.	Recombinant apoferritin used. Binding peptide genetically fused to the surface of recombinant apoferritin.	Magnetism showed. MRI experiments have been performed.	(Uchida *et al.*, 2006; Uchida *et al.*, 2008)
	Magnetic.	Recombinant apoferritin from thermophilic bacterium *Pyrococcus furiosus.*	Particles showed enhanced magnetic properties to previous ones (due to possibly different interior from mammalian ferritins).	(Parker *et al.*, 2008)
Lead sulfide (PbS) particles.	Photoluminescent particles, near-infrared.	Apoferritin from horse spleen ferritin used.	Produced particles within ferritin are inherently photoluminescent.	(Hennequin *et al.*, 2008), Two separate loading methods (another below)

Lutetium phosphate.	Model for radionuclide Lutetium-177 that has potential medical applications.	Horse spleen apoferritin used.	N/A.	(Wu *et al.*, 2008)
Manganese oxide/ oxyhydroxide particles.	N/A.	Both recombinant apoferritins and apoferritin made of horse spleen ferritin were used.	N/A, a basic loading mechanism study.	(Meldrum *et al.*, 1995; Meldrum *et al.*, 1991)
Nickel particles.	Possibly usable in nanoelectronics.	Both horse spleen apoferritin and recombinant apoferritin used.	N/A.	(Okuda *et al.*, 2003)
Palladium complexes.	Catalytic.	Recombinant apoferritin used.	Catalytic reactions were shown.	(Abe *et al.*, 2008)
Phosphate particles from cadmium, zinc, or lead. Alternatively, mixtures of different phosphates in single particle.	Released metal ions can be detected voltammetrically.	Horse spleen apoferritin used.	Loaded apoferritin surface chemically biotinylated. Particles used as labels in electrochemical immunoassay.	(Liu *et al.*, 2007; Liu *et al.*, 2006c) Two loading methods demonstrated (see below)
Silver (metallic) particles.	Surface plasmon resonant particles.	Recombinant apoferritin used. Apoferritins were mutated to possibly optimize the loading.	Surface plasmon resonance of the particles shown.	(Butts *et al.*, 2008)
Uranyl oxyhydroxide.	N/A.	Apoferritin from horse spleen ferritin used.	N/A, preliminary study.	(Meldrum *et al.*, 1991)
Uranium (oxide) particles	Radioactive ferritin (in a neutron beam). Suggestion as radio-pharmaceuticals.	Commercial horse apoferritin used.	Antibody Fab-fragments chemically coupled to the protein cage.	(Hainfeld, 1992)
Zinc selenide (ZnSe) particles.	Semiconducting particles used in nanoelectronics and photoluminescence	Recombinant apoferritin used.	Weak photoluminescence shown. (Weakness due to polycrystallinity of ZnSe)	(Iwahori *et al.*, 2005)

Loading methods that are based on transforming core of ferritin or on reactions of ferritin core.				
Iron sulfide-coated iron oxide particles.	N/A.	Horse spleen ferritin was used.	Slight magnetism shown by St. Pierre *et al.* 1993. (Color, black)	(Meldrum *et al.*, 1991; St. Pierre *et al.*, 1993)
Iron sulfide particles.	N/A.	Horse spleen ferritin was used.	N/A (Color, green).	(Douglas *et al.*, 1995)
Loading methods that are based on first diffusion of the ions and then transformation of the core material.				
Cisplatin.	Anticancer drug.	Apoferritin from horse spleen ferritin was used.	Preliminary cytotoxicity has been demonstrated.	(Yang *et al.*, 2007)
Cu particles.	N/A.	Horse spleen apoferritin was used.	N/A (Color, yellow).	(Galvez *et al.*, 2005)
CuFe particles.	Magnetic.	Horse spleen apoferritin was used.	N/A (Color, red-brown).	(Galvez *et al.*, 2005)
Cobalt and nickel particles.	Magnetic.	Horse spleen apoferritin was used.	Some magnetism was shown.	(Galvez *et al.*, 2006)
Cobalt platinum (CoPt) particles.	Magnetic.	Apoferritin from commercial ferritin used.	Proper magnetism was shown with ferritin coat removed.	(Warne *et al.*, 2000)
Palladium (metallic).	Catalytic.	Apoferritin from horse spleen ferritin used.	Loaded ferritin particle used in size-selective olefin hydrogenation.	(Ueno *et al.*, 2004)
Silver (metallic) particles.	Surface plasmon resonant particles.	Horse spleen apoferritin used.	Surface plasmon resonance was shown.	(Dominguez-Vera *et al.*, 2007)
Loading methods that are based on using peptides for inorganics.				
Ag (metallic) particles.	N/A.	C-terminal template peptide used for generating particles inside recombinant apoferritin.	N/A.	(Kramer *et al.*, 2004)
CoPt particles.	Magnetic particles.	Preparation as above.	N/A.	(Kramer *et al.*, 2004)

Loading methods that are based on denaturation-refolding of apoferritin.				
Entrapment of pH indicator molecules.	pH indicator	N/A.	N/A, used for studying ferritin.	(Webb *et al.*, 1994)
Entrapment of gadolinium complexes.	Magnetic particles, Potential as MRI contrast agent.	Commercial apoferritin used.	MRI experiments have been performed (*in vitro* and *in vivo*).	(Aime *et al.*, 2002b; Geninatti Crich *et al.*, 2006)
Hexacyanoferr -ate particles.	Potential as marker molecule.	Horse spleen apoferritin used.	Addition of Fe resulted in a blue color ("Prussian blue").	(Dominguez-Vera and Colacio, 2003)
	Potential as marker molecule.	Horse spleen apoferritin used.	Particles used as labels in electrochemical immunoassay.	(Liu *et al.*, 2006a; Liu *et al.*, 2006b)
Entrapment of doxorubicin molecules.	Potential anticancer drugs within ferritin.	Horse spleen apoferritin used.	N/A.	(Simsek and Kilic, 2005)
Entrapment of fluorescein.	Fluorescent particles.	Horse spleen apoferritin used.	Particles used as labels in immunoassay.	(Liu *et al.*, 2006b)
Entrapment of methylene blue.	The compound acts as photosensitizer: Potential use in photodynamic therapy of cancer.	Horse spleen apoferritin used.	Cytotoxicity has been demonstrated	(Yan *et al.*, 2008)
Entrapment of cisplatin and carboplatin	Anticancer drugs.	Apoferritin from horse spleen ferritin was used.	Cytotoxicity has been demonstrated.	(Yang *et al.*, 2007)
Entrapment of PbS particles.	Photoluminescent particles, near-infrared.	Apoferritin from horse spleen ferritin was used.	Particles entrapped by apoferritin are inherently photoluminescent; no need for heat treatment.	(Hennequin *et al.*, 2008)

Mechanisms of metallic nanoparticle formation inside apoferritin have not received much attention. However, it is hypothesized that many different reactions are involved, in which components form metallic cores under specific conditions. These reactions don't presumably involve ferritin heavy chain ferroxidase activity because it is mainly involved only in loading of small ions but additional oxidants, such as H_2O_2, are used to permit oxidative hydrolysis if that is needed. Also, several different ions can be added simultaneously or sequentially, thus generating materials other than typical metal hydroxides or oxides (Douglas and Stark, 2000; Liu *et al.*, 2006c; Wong *et al.*, 1998). In general, the theory behind such processes assumes that metal ion binding sites are present on the inner surface of the protein cage, based on (for example) electrostatic forces. These sites probably act as startpoints for mineralization reactions (*e.g.,* autoxidation), which proceed further on the surfaces of incipient metal particle seeds

(Figure 10A). Incipient particles probably grow, and further merge, on the surface of the apoferritin cavity, thereby forming multinucleate single particles (Kim *et al.*, 2005). Exceptions have been, however, reported. Indium oxide particles have presumably grown from a single nucleation point thus forming exceptionally homogeneous particles inside apoferritin (Okuda *et al.*, 2005). These metal loading approaches offer the possibility of fine-tuning metallic particle size within ferritin cage by varying the proportions of added substances in the reactions. Size-tunability is important in (for example) semiconducting and magnetic nanoparticles. (Dominguez-Vera *et al.*, 2007; Gider *et al.*, 1995; Hosein *et al.*, 2004; Uchida *et al.*, 2006) When encapsulation methods are used (Figure 10C), molecules are typically passively loaded into apoferritin.

In summary, various compounds have been introduced into ferritin, apoferritin, and ferritin-like proteins (Table 1). Metal aggregates in bulk solution have rarely been formed if precursor compounds have been added at near-stoichiometric amounts. The typical method for study of apoferritin loading has been transmission electron microscopy (TEM) because metal particles formed can often be visualized and differentiated from the protein coating, thus directly showing loading efficiency. Also, chromatographic methods combined with spectroscopic analysis have been employed. Detailed analyses of metal particles are based on energy-dispersive X-ray approaches that reveal the compositions of metal particles as well as possible crystal structures. Reported apoferritin particle loading efficiencies, where mentioned, have been 50-90%, depending largely on metal particle type (Kramer *et al.*, 2004; Meldrum *et al.*, 1995; Okuda *et al.*, 2003; Yamashita *et al.*, 2006; Yoshizawa *et al.*, 2006). Thus, further efforts may be needed to optimize several loading methods, depending on the final particle application. Additionally, discovery of optimal loading conditions may not be trivial, and at least some reactions require particular conditions, and thereby extensive experimental optimization (Okuda *et al.*, 2003). Parameters to be investigated may include reaction atmosphere, pH, temperature, buffer type, possible need for additional ions for compound synthesis, any need (using polymers or chelators) for inhibition of excessively fast reactions leading to non-specific metal aggregation, and any requirement for enhancers (*e.g.,* additional reducers or oxidants) of ferritin function (Ensign *et al.*, 2004; Li *et al.*, 2007; Okuda *et al.*, 2003; Okuda *et al.*, 2005).

The characteristics and potential functions of loaded ferritins, or of particles produced using apoferritin protein cages, are many. Colored, semiconducting, magnetic, catalytic, and fluorescent particles have been formed (Table 1). Metallic compounds/particles have been loaded inside ferritin with two intentions. First, ferritins are used as “particle reactors” to form size- and shape-constrained metallic particles, possibly aiding in particle targeting to desired surfaces. Such applications often include removal of the ferritin protein coating, for example by pyrolysis at temperatures above 400°C under nitrogen gas (Iwahori *et al.*, 2005; Takagi *et al.*, 2007; Yamashita *et al.*, 2006). Sometimes this heat treatment is necessary before a metal particle shows desired properties such as efficient photoluminescence or particular magnetic properties, which are compromised by the multinucleate character of apoferritin-generated metal particles (Figure 10A). The heat treatment transforms particles to single crystals and simultaneously removes ferritin cage (Galvez *et al.*, 2006; Hosein *et al.*, 2004; Iwahori *et al.*, 2005; Warne *et al.*, 2000). Secondly, in some potential applications both the apoferritin cage

and the material inside are utilized. The protein cage has made metallic particles, in particular, water-soluble, and minimized non-specific aggregation of such particles (Yoshizawa *et al.*, 2006). In addition, the protein coating offers possibilities for various further particle modifications (*e.g.*, bioconjugation). Recently, inherently photoluminescent PbS particles were successfully created within apoferritin. Two methods were described, and there was no need for heat treatment, thus enabling also utilization of the protein cage (Hennequin *et al.*, 2008).

4.3 Modifications of ferritin nanocontainers

Most methods described in Table 1 have used commercial ferritins (mostly equine) with only a few examples of recombinant ferritins. Ferritins actually loaded or potentially loadable with different molecules have additionally been modified by chemical means and recently also utilizing recombinant gene technology.

Chemical reactions exploiting free amino and carboxyl groups on the surface of ferritin nanocontainers have been used to add further functionalities, such as specific binding activities (*e.g.,* biotin, or mononucleotides) or label activities (*e.g.,* fluorescent molecules conjugated to the ferritin surface) (Fernandez *et al.*, 2008; Fernandez *et al.*, 2007; Li *et al.*, 1999; Liu and Lin, 2007; Wu *et al.*, 2008). Another purpose of chemical modifications has been to modify chemico-physical characteristics of ferritin. For example, ferritins with chemically altered surface charges (*i.e.,* cationic ferritins) have long been used to visualize oppositely charged spots on various cells in TEM and recently also as charge-specific contrast agents in magnetic resonance imaging (MRI) (Bennett *et al.*, 2008; Danon *et al.*, 1972). By conjugating hydrophobic molecules onto ferritin the hydrophilic nature of the surface is altered thus enabling ferritins to be dissolved in hydrophobic solvents. This may extend ferritin loading possibilities in reactions requiring organic solvents, and may impart self-directing properties to ferritin in polymer solvents, which could permit (for example) controlled multistage drug release (Sengonul *et al.*, 2007; Wong *et al.*, 1999). Actual applications along these lines have not, however, been reported.

There are few reports on use of recombinant gene technology to load ferritin with alternative substances. As mentioned earlier, a straightforward and promising approach to expand the spectrum of ferritin-binding specificities includes fusion of ferritin subunits to peptides specific for certain metals (such as Ag or CoPt) or other molecules, and located inside apoferritin. Alternatively, this method has been used to add specific binding activities (for carbon nanotubes, cell markers, and metals) to the outer surface of apoferritin (Hayashi *et al.*, 2006; Kramer *et al.*, 2004; Sano *et al.*, 2005; Uchida *et al.*, 2006; Yamashita *et al.*, 2006). As peptide specificity can be relatively easily modified using *in vitro* display methods, the possibilities are vast (Whaley *et al.*, 2000). Recently, efforts to genetically modify the inner surface of the ferritin protein cage to make the cage more (or less if desired) attractive to particular ions or molecules have been reported. The goals of the studies have been to control the numbers of nucleation points inside apoferritin or optimizing apoferritin loading by amino acid changes and to make the negative inner surface of ferritin suitable for acceptance of hydrophobic molecules (Abe *et al.*, 2008; Butts *et al.*, 2008; Swift *et al.*, 2006).

5 Ferritin in biomedical applications

Even though research on ferritin loading with various compounds has been vigorous, research groups demonstrating actual biomedical applications of ferritin have been relatively few. Only in recent years ferritin has been employed in biological applications, even though early suggestions on biomedical uses of ferritin (for example as a "magic bullet" to transport an anticancer activity in humans) appeared already in the early 1990s (Hainfeld, 1992). Recently, preliminary experiments *in vitro* have shown potential cytotoxicity of drug-loaded ferritins (Yan *et al.*, 2008; Yang *et al.*, 2007).

5.1 Bioaffinity assays utilizing ferritin as a reagent

Lin's group has developed various bioaffinity assays, in which specific target molecules have been quantitatively detected *in vitro*. The assay systems have thus produced signals proportional to amount of the target molecule. Detection has been based on bifunctionalized apoferritin particles. For these assays, horse spleen apoferritin was loaded with various marker molecules and the ferritin surface chemically functionalized to show affinity toward target molecules.

Work has included development of both fluorescence (using fluorescein) and electrochemical detection technologies. The marker hexacyanoferrate [$K_3Fe(CN)_6$] was first employed as an electrochemically detectable material and later on, metallic phosphate particles (phosphates of Cd^{2+}, Zn^{2+}, and Pb^{2+}) competing with semiconducting quantum dots were introduced. Quantum dots of these cations can also be detected electrochemically but require harsh conditions to release metal ions prior to the measurement, unlike respective phosphates (Liu *et al.*, 2007; Wang *et al.*, 2003). Different metal ions have different potentials in which they produce measurable currents and the current intensities are related to ion levels. Lin and others have succeeded also in producing bimetallic Cd^{2+} and Pb^{2+} phosphate particles inside apoferritin. The current intensities obtainable with such particles correlate with the proportions of each metal in the particles, which is controllable by proportions of cations used in preparation of particles. Therefore, ferritin-based nanoparticles with individual detection codes can be made using this method because the detection codes depend on the metals used, and their proportion in the material. This enables assay multiplexing, which means that multiple targets can be simultaneously detected in a single assay by using various specific particles (Liu *et al.*, 2007; Liu *et al.*, 2006c). Binding molecules (*e.g.,* biotin, oligonucleotides, antibodies) have been chemically conjugated to loaded apoferritin surfaces to enable particle binding to target molecules. Assay performances, such as detection sensitivities for proteins or single nucleotide polymorphisms (SNP) have been stated to be equal to or even better than those of conventional assays (Liu and Lin, 2007; Liu *et al.*, 2006a; Liu *et al.*, 2006b; Liu *et al.*, 2007; Liu *et al.*, 2006c).

Lee's group have used genetically modified recombinant ferritins in bioaffinity assays to capture target antibodies on a solid surface (Lee *et al.*, 2007). In such applications, various antigens have been genetically fused to the C-terminal end of the heavy-chain ferritin subunit. Thus, ferritin has been forced into the "flop" conformation, in which the C-terminal ferritin end

points to the outer surface of ferritin instead of to the cavity interior even though this compromises particle stability (see Section 3.2) (Choi *et al.*, 2005; Lee *et al.*, 2007). Ferritin particles displaying surface antigens were bound to a solid surface (a membrane), on which they captured target antibodies. Two detection mechanisms were used. One was PCR-based, and the other involved labeled antibodies conjugated to highly photoluminescent commercial quantum dots. Different antibodies (*e.g.,* diabetes autoantibodies and hepatitis B antibody) could be detected using this rather complicated assay procedure, with high sensitivities for both antibody types. Additionally, assay multiplexing has been demonstrated (Lee *et al.*, 2007).

5.2 Potential *in vivo* applications of ferritin

Progress in medical imaging technologies such as MRI has drawn attention of researchers. In addition to a role as improved contrast agents for MRI, magnetic particles can be useful in cancer therapy (hyperthermia treatment of cancer cells). The use of two types of ferritin-based magnetic materials have been demonstrated in preliminary biomedical applications; these materials are iron oxides and paramagnetic gadolinium chelates.

Gadolinium chelates incorporated in the ferritin cavity using the pH encapsulation method (Figure 10C) have shown magnetic effects superior to those of free chelates in water, as represented by conventional contrast agents (Aime *et al.*, 2002b). It has been suggested that the observed enhancement is related to the presence of multiple chelates in a single ferritin particle, and to an interaction between the paramagnetic chelates and protein surface of the ferritin cavity (Aime *et al.*, 2002b; Vasalatiy *et al.*, 2006). An additional advantage of ferritin is the possibility to modify the protein coat to assist in directing the contrast agent to specific organs or cells, facilitating molecular visualization by improved, targeted responses (Aime *et al.*, 2002a; Geninatti Crich *et al.*, 2006). Chemically biotinylated apoferritin, loaded with gadolinium complexes (8-10 chelates/protein shell), have been shown to concentrate in desired pre-targeted cells (tumor endothelial cells) both *in vitro* and *in vivo* in mice with Severe Combined Immunodeficiency (SCID) (Geninatti Crich *et al.*, 2006).

Creating of magnetic iron oxide particles (magnetite or maghemite) inside ferritin was described in the early 1990s (Meldrum *et al.*, 1992), and the loading method was refined thereafter (Uchida *et al.*, 2006; Wong *et al.*, 1998). The loading of iron oxide mimics normal iron mineralization by ferritin but different reaction conditions are employed. Thus, loading is performed under N_2 at temperatures above 60°C using H_2O_2 as an additional oxidant. The use of such magnetic ferritin particles in cells has been demonstrated in recent years. Cancer cells have been specifically targeted using recombinant human ferritin with N-terminal targeting peptides on the ferritin surface and internal magnetic iron oxide; even though cancer cells also have some receptors for wild-type ferritin (Fargion *et al.*, 1988; Uchida *et al.*, 2006). Macrophages were also visualized by MRI using non-targeted ferritins loaded with magnetic iron oxide, and the MRI performance of ferritin-coated iron oxide was determined to be comparable to or even better than current commercial iron oxide MRI contrast agents (Uchida *et al.*, 2008).

Ferritin particles may offer targeting possibilities *in vivo*, presumably non-toxicity, and biocompatibility. However, biodistribution and toxicity have not yet been examined in detail.

When human-like ferritin proteins are microbially generated, the lack of possible eukaryotic post-translational modifications (Zaman and Verwilghen, 1981) may affect functions in humans. Also, effects of ferritin functionalizations, such as targeting moieties and associated markers or therapeutic agents need to be considered.

6 Aims of the study

The overall aim of the study was to develop a novel production system for functionalized nanoparticles used in bioaffinity assays. The specific aims were as follows:

(1) Design of ferritin cage-based particles that contain a marker substance and display binding molecules on the surface. Production of functional particles should follow principles of “green chemistry”.

(2) Establishment of a simple biological production system for functional ferritin-based nanoparticles, offering the possibility for easy upscaling of the production, including purification of the particles.

(3) Demonstration of the utility of the functionalized particles in bioaffinity assays, with reference to contributions made by binding molecules and marker agents.

These goals were pursued by genetically fusing genes encoding binding molecules and a ferritin subunit, and by microbial particle material production. The non-chromatographic purification procedure was straightforward, including self-assembly of particles with surface binding molecules, during which the marker molecules were introduced. This system can be easily upscaled and bacterial fermentation complies with the principles of green chemistry.

7 Materials and Methods

The human ferritin light chain was used because this chain is more stable than the heavy chain subunit (Santambrogio *et al.*, 1993). The ferritin-based particles produced are called hereafter as ferritin even though the particles contained no iron. Three different binding molecules were chosen for analysis. The first was Biotin Carboxyl Carrier Protein, BCCP, a small protein of 87 amino acids, that becomes biotinylated in *E. coli* cells (Cronan, 1990), thereby generating particles with an inherent ability to bind streptavidin (Figure 11A) (Wilchek and Bayer, 1999). The second was a single-chain antibody fragment (scFv), a complex binding protein, enabling the production of particles inherently specific for a desired analyte (Figure 11B). The scFv protein contains the variable parts of antibody heavy and light chains joined by a linker, and stabilized by a disulfide bridge, to form a single polypeptide chain (Bird *et al.*, 1988). The third binding molecule was the 27-amino acid calmodulin-binding peptide, CBP, which binds to calmodulin in the presence of approximately 2 mM Ca^{2+} (Neri *et al.*, 1995). Calmodulin can be genetically fused to any binding moiety, such as an antibody fragment, and particles of desired specificity can be generated by associating CBP-ferritin with a fusion protein including calmodulin and a binder molecule (Figure 11C). The model antibody fragment used here, scFv, is directed against thyroid-stimulating hormone (TSH), and is termed αTSHscFv (Brockmann *et al.*, 2005). This protein was directly fused to either ferritin or calmodulin.

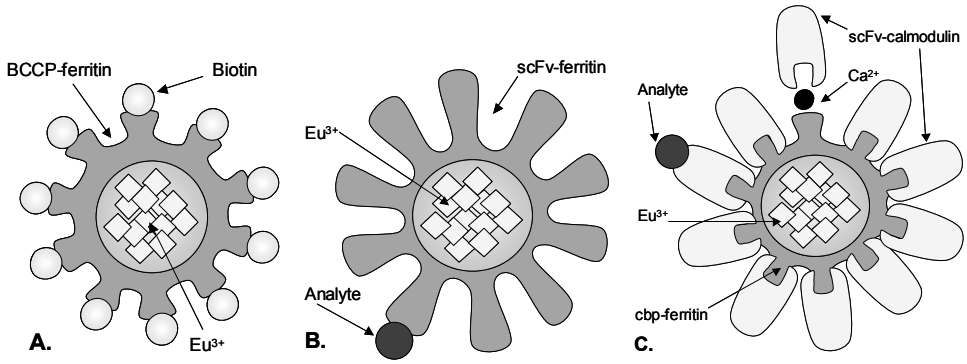

Figure 11. Ferritin-based nanoparticles containing different types of surface binding molecules and Eu^{3+} ions as fluorescent markers. A. BCCP-ferritin. Biotin carboxyl carrier protein, BCCP, is a small protein that is biotinylated in *E. coli* cells. Consequently, the particles are able to bind streptavidin and further any biotinylated molecules. B. αTSHscFv-ferritin contains, on the ferritin surface, an antibody fragment specific for thyroid stimulating hormone (TSH). Such particles are inherently TSH-specific. C. Calmodulin-binding peptide (CBP)-ferritin. CBP binds calmodulin in the presence of Ca^{2+} ions. Calmodulin can be fused to many binding molecules, such as scFv. TSH-specific scFv was associated with calmodulin. Figure modified from publication III.

The different binding moieties permit various particle applications. The scFv can be used to directly produce particles specific for desired analytes; BCCP enables particle use in (strept)avidin-biotin technology; CBP-displaying particles can be linked to antibodies (or other

binding molecules) of any specificity, via calmodulin, to create modular systems. When particle label functionality was required, Eu^{3+} ions were used as an inorganic label because these ions can be detected at very low levels using time-resolved fluorometry. The technology has been reviewed in Hemmilä and Mukkala (2001). The use of both Eu^{3+} and binding molecules should make the particles suitable as labels in bioaffinity assays. Particles without label may be used in particle-enhanced agglutination assays.

All details of materials and methods have been published in original research papers. Here, the methods used are described in general.

7.1 Gene fusions and particle production

The 3' ends of genes encoding the desired binding molecules were fused with the 5' end of the human ferritin light chain gene because the amino-terminal ends of ferritin subunit chains are located on the outer surface of ferritin. Thus, the binding molecules will point out to the solution.

The process for generating ready-to-use particles with surface binding molecules and Eu^{3+} ions as a marker is outlined in Figure 12. Production involved bacterial cultivation. Fusion polypeptides consisting of the binding moiety and the ferritin subunit were produced as inclusion bodies within *E. coli*. Particle purification commenced with inclusion body isolation; this was easily achieved using generic procedures (*i.e.,* washing with detergent followed by optional sonication and centrifugation). Next, the inclusion bodies were dissolved at low pH or in 8 M urea and released polypeptides were allowed to self-assemble by raising the pH gradually or by diluting the urea solution 10-fold (Figure 12). This forms globular nanoparticles with surface binding activities (Figure 11). When desired, particle labeling was achieved by introducing Eu^{3+} ions before the self-assembly step.

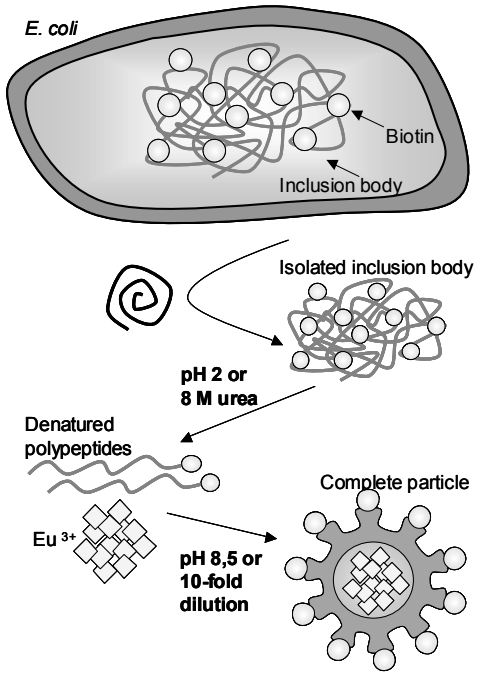

Figure 12. The production-purification process of particles using BCCP-ferritin as a model particle. BCCP-ferritin fusion polypeptide chains were produced as inclusion bodies in *E. coli* containing a plasmid expressing the fusion gene *BCCP-FtL*. Inclusion bodies were purified from cell lysates by two steps of centrifugation, sonication (optional), and washing (denoted with a spiral). Inclusion bodies were solubilized at pH 2.0 or in 8 M urea, and the particles reassembled when the pH was gradually raised to pH 8.5, or urea was diluted 10-fold. To label the particles, 0.6 μM $EuCl_3$ was added to solutions when the pH was below pH 6.0. Figure modified from publication I.

7.2 Particle characterization

In general, protein yields were determined by SDS-PAGE analysis, or using a ferritin immunoassay with wild-type ferritin as standard. This can be done when the binding moiety on the ferritin surface is considered sufficiently small to permit anti-ferritin antibodies to recognize the fusion ferritins. The immunoassay scheme is shown in Figure 13A. Purification efficiencies were qualitatively estimated from SDS-PAGE gels. Additionally, the formation of BCCP-ferritin particles was studied by TEM.

The functionalities of binders fused to ferritin were determined in bioaffinity assays using ferritin particles without loaded Eu^{3+}. The assay schemes for each particle type are presented in the Figures that follow. Figure 13B shows the bioaffinity assay determining the streptavidin-binding activity of biotin-displaying BCCP-ferritin particles, using labeled streptavidin. For both αTSH-ferritin and CBP-ferritin, correct folding of binding molecules on the ferritin surface was confirmed using biotinylated and Eu^{3+}-chelate-labeled TSH (Figure 14).

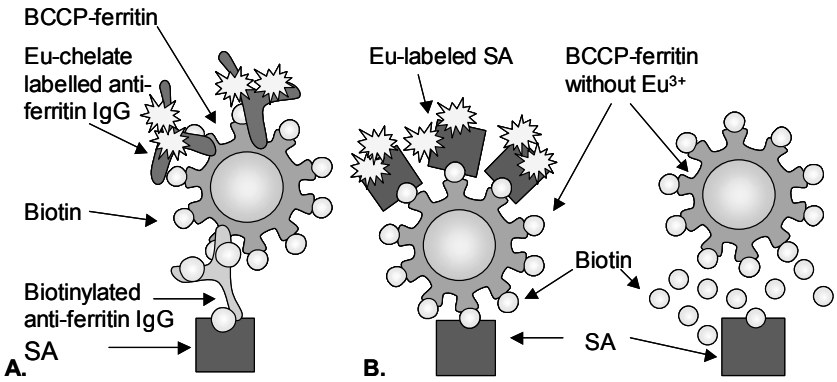

Figure 13. Assays used to examine BCCP-ferritin particles. A. An immunoassay for ferritin. Biotinylated anti-ferritin antibodies were bound to streptavidin-coated microtiter wells. After removal of unbound antibody by washing, BCCP-ferritin was added to the wells. After incubation, Eu^{3+}-chelate-labeled anti-ferritin antibody was added. Unbound ferritin and antibody were removed by washing and Eu^{3+} fluorescence measured. B**.** Streptavidin binding assay. Biotin-displaying BCCP-ferritin particles were added to streptavidin-coated microtiter wells. To measure non-specific particle binding, specific binding was inhibited by saturating some streptavidin-coated wells with free biotin. After removal of unbound particles, Eu^{3+}-chelate-labeled streptavidin was added. Unbound streptavidin was removed and Eu^{3+} fluorescence measured. SA=streptavidin. Figure modified from publication I.

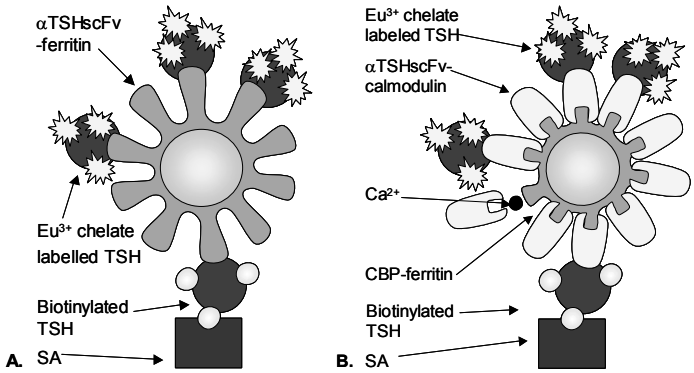

Figure 14. TSH-binding activities of particles lacking Eu^{3+}. A. The TSH-binding activity of αTSHscFv-ferritin was assessed using biotinylated and Eu^{3+}-chelate-labeled TSH. αTSHscFv-ferritin particles were attached to a solid surface containing biotinylated TSH. After removal of unbound particles, TSH labeled with Eu^{3+}-chelate was added. Unbound labeled TSH was removed and fluorescence was measured. B. The TSH-binding activity of CBP-ferritin combined with αTSHscFv-calmodulin was evaluated as described above (in A) for αTSHscFv-ferritin. αTSHscFv-calmodulin was associated with CBP-ferritin in the presence of Ca^{2+} before addition of particles to the assay. The negative controls for the assay were CBP-ferritin without αTSHscFv-calmodulin and αTSHscFv-calmodulin combined with wild-type ferritin. In addition to TSH-binding, the calmodulin-binding activity of CBP on the surface of ferritin was measured. SA=streptavidin. Figure modified from publication II.

7.3 Use of particles in bioaffinity assays

Functionalities of the produced nanoparticles were demonstrated in bioaffinity assays. Particles (BCCP-ferritin, αTSHscFv-ferritin, and CBP-ferritin) loaded with Eu^{3+} ions, were used in heterogeneous assays (*i.e.*, assays including separation steps) as shown in Figure 15. The assays utilized solid carriers (*e.g.,* a. microtiter well) which enabled excess, unbound reagents to be removed by washing. Fluorescence specific for the target molecule (biotinylated IgG or TSH), from Eu^{3+} ions, was detected using DELFIA™ technology (Perkin-Elmer Life Sciences, Turku, Finland). Eu^{3+} fluorescence was developed using dissociating fluorescence enhancement solution that has low pH (pH 3.5) and that contains materials dissociating Eu^{3+} ions from particles. The chelates in solution form highly fluorescent chelates with released Eu^{3+}. The fluorescence of the Eu^{3+} chelates can be measured in a time-resolved manner. For a review of the technology, see Hemmilä and Mukkala (2001)

BCCP-ferritin without Eu^{3+} was also tested in particle-enhanced agglutination assays (Figure 16). Ferritin nanoparticles coated with specific binding molecules (*e.g.,* BCCP linked to biotin) were agglutinated with appropriate amounts of a target molecule (streptavidin) with multiple biotin-binding sites. The agglutination reaction was spectrophotometrically quantified by detecting light dispersion by the aggregates. Also, agglutination products were visualized by TEM.

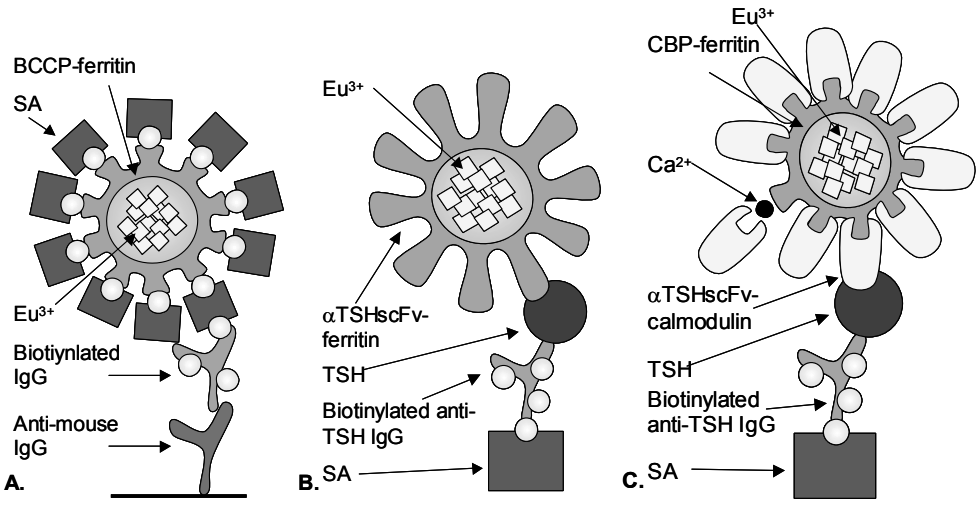

Figure 15. Functionality of ferritin-based nanoparticles used as label agents in bioaffinity assays. A. BCCP-ferritin was used to detect biotinylated antibody. The biotinylated antibody bound to anti-mouse-IgG-coated microtiter wells. Unbound antibody was removed by washing. BCCP-ferritin was mixed with streptavidin and added to the wells. After removal of excess particles by washing, Eu^{3+} fluorescence was measured. B. αTSHscFv-ferritin was used to detect TSH. Biotinylated monoclonal antibody against TSH was attached to a streptavidin-coated solid surface. Unbound antibody was removed by washing, and TSH was added to the wells. Following the removal of unbound TSH, αTSHscFv-ferritin particles containing Eu^{3+} were added. Unbound particles were removed and Eu^{3+} fluorescence measured. C. CBP-ferritin containing Eu^{3+} and combined with αTSHscFv-calmodulin was measured by using the particles as

labeling agents in an assay for TSH, as described above (in B) for αTSHscFv-ferritin. αTSHscFv-calmodulin was associated with CBP-ferritin in the presence of Ca^{2+} before particle use. SA=streptavidin. Figure modified from publications I-III.

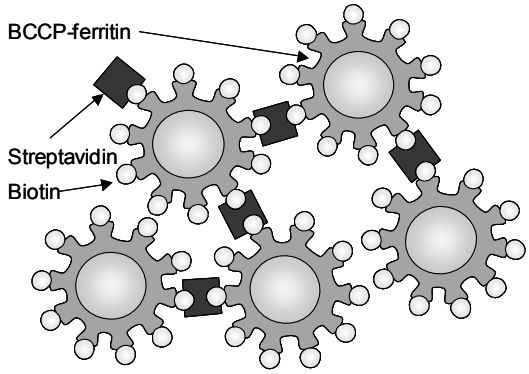

Figure 16. Particle-enhanced agglutination assay using BCCP-ferritin particles devoid of Eu^{3+} ions. Because streptavidin has four biotin-binding sites, streptavidin cross-links biotin-displaying BCCP-ferritin particles, creating aggregates. The sample (streptavidin) was added to biotin-displaying-ferritin. Reactants were mixed briefly and incubated at room temperature for 5 minutes. The absorption spectrum of the agglutination product was measured. Figure modified from manuscript IV.

8 Summary of Results

8.1 Bacterial production and purification of the proteins

The extent of bacterial production of fusion ferritin subunits (Figure 11), and the effective purification of such proteins, were examined by SDS-PAGE performed after purification and denaturation-refolding employing both the urea and pH methods. Inclusion bodies of BCCP-ferritin were purified with a protocol utilizing sonication but sonication was omitted during purification of αTSHscFv-ferritin and CBP-ferritin.

SDS-PAGE of BCCP-ferritin revealed the presence of a fusion polypeptide of the appropriate size (29.7 kDa) (Figure 17A). Both particle preparations were pure but particles generated using the pH refolding method contained less contaminating proteins than did those produced with the urea method, even though urea-refolded particles were five-fold more dilute than were pH-refolded particles.

SDS-PAGE analysis of αTSHscFv-ferritin fusion polypeptides, produced using both refolding methods, revealed bands corresponding to the fusion polypeptide (47.3 kDa) (Figure 17B and 7C), and bands corresponding to CBP-ferritin polypeptides were also clearly visible at 23.5 kDa (Figure 17D). Remarkably few contaminating proteins were detected considering the simple purification procedure used (no sonication was employed during isolation of inclusion bodies). Two contaminating bands may be detected by comparison with the SDS-PAGE tracks of BCCP-ferritin, the inclusion bodies of which had been purified using sonication (Figure 17A).

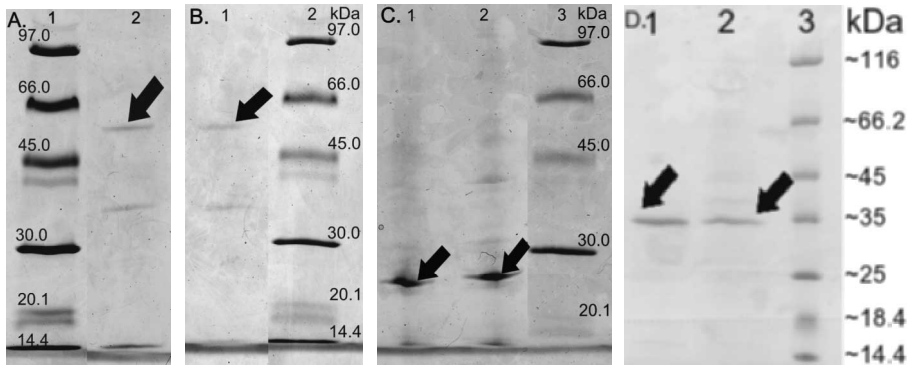

Figure 17. SDS-PAGE gels of ferritin fusion polypeptides produced by both pH and urea denaturation-refolding methods. Gels were run after production, purification, and self-assembly of subunits to create the final particles. A. αTSHscFv-ferritin produced by pH method. Lane 1: molecular weight calibration protein mixture; lane 2: polypeptides resulting from fusion of αTSHscFv and the ferritin subunit. The arrow indicates αTSHscFv-ferritin subunits (47.3 kDa). B. αTSHscFv-ferritin produced by urea method. Lane 1: fusion polypeptide; lane 2: molecular weight calibration protein mixture. The arrow indicates αTSH-ferritin. C. CBP-ferritin fusion polypeptides produced by the pH and urea methods. Lanes 1 and 2: CBP-ferritin produced by pH and urea denaturation-refolding, respectively; lane 3: molecular weight calibration protein mixture. The arrows indicate CBP-ferritin subunits (23.5 kDa). D. Lanes 1 and 2: BCCP-ferritin generated by the pH and urea denaturation-refolding methods, respectively, showing BCCP-ferritin polypeptides of appropriate size (29.7 kDa). Lane 3: molecular size standard mixture.

The yield of BCCP-ferritin in bacterial production was estimated by immunoassay using wild-type ferritin as a standard (Figure 3A). The yield of BCCP-ferritin particles was on average 2.3 mg/l and 6.5 mg/l of bacterial culture medium when the pH and urea denaturation-refolding methods, respectively, were used. By varying refolding conditions (setting the pH to 8.5, adding reduced glutathione, and raising the pH gradually) the refolding yield was improved to 11 mg/l. BCCP-ferritin particles were also produced in two different *E. coli* strains [BL21(DE3)pLysS and BL21(DE3)] and at two different temperatures (37ºC and 26ºC); production conditions affected both particle yield and the extent of biotinylation. Strain BL21(DE3)pLysS expresses T7 lysozyme; the enzyme slightly inhibits T7 RNA polymerase, and thus slows expression of the desired gene (*BCCP-ferritin*). This probably affords BCCP more biotinylation time prior to folding into inclusion bodies.

The yields of αTSHscFv-ferritin and CBP-ferritin were calculated from the SDS-PAGE gels. αTSHscFv-ferritin particles were produced at yields of 4.4 mg/l and 1.1 mg/l of culture medium urea and pH denaturation-refolding methods, respectively. CBP-ferritin yields with the urea and pH methods were 42.3 mg/l and 9.3 mg/l of culture medium, respectively.

Overall, yields from the urea and pH denaturation-refolding methods, and levels of contaminating proteins seen, were similar for all ferritin fusions. The results indicated that urea denaturation-refolding was the gentler method for releasing polypeptides from inclusion bodies. Use of urea improved particle concentration but increased the amount of contaminating proteins.

8.2 Characterization of particles

8.2.1 Particle formation

The formation of BCCP-ferritin particles was examined by TEM, and the particles were homogenous (Figure 18A). Compared to wild-type ferritin particles (Figure 18B), the surfaces of BCCP-ferritin particles (Figure 18A) were sometimes studded with small spikes. These are probably BCCP molecules protruding from the particle surface. As BCCP is rather small, its appearance varies and depends on the amount of staining solution remaining around the particles.

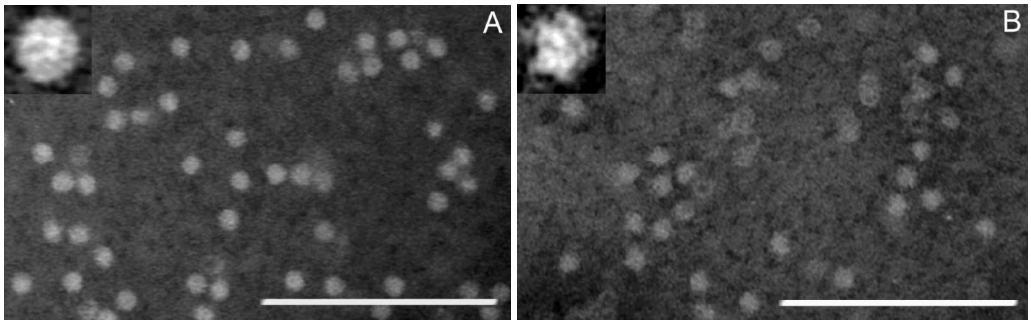

Figure 18. TEM images of (A) BCCP-ferritin and (B) wild-type ferritin particles. Both samples are negatively stained with phosphotungstic acid (PTA; 0.5%, w/v). The scale bars are 100 nm. The insert shows single particles at higher magnification.

8.2.2 Activities of binding molecules

Functionalities (binding activities) of molecules on the ferritin surface were demonstrated using bioaffinity assays with particles not loaded with Eu^{3+}. The ability of BCCP-ferritin particles to bind the target streptavidin was determined by attaching BCCP-ferritin particles to streptavidin-coated plates, followed by detection with Eu^{3+} chelate-labeled streptavidin (Figure 13B). BCCP-ferritin produced by pH denaturation-refolding was employed. To determine the extent of nonspecific binding, specific binding was inhibited by saturating solid-phase streptavidin with soluble biotin (Figure 13B). The results show specific streptavidin-binding activity of BCCP-ferritin particles (Table 2).

Table 2. Specific streptavidin-binding activity of BCCP-ferritin particles.

-Fold dilution	Specific binding		Nonspecific binding[b]	
	Fluorescence (RFU)[a]	CV% (n=2)	Fluorescence (RFU)[a]	CV% (n=2)
100	372058	6	9195	16
1000	37833	3	2209	61
10000	2021	2	679	11

[a] RFU, Relative fluorescence units.
[b]Nonspecific binding indicates binding of the labeled streptavidin to microtiter wells that did not contain bound BCCP-ferritin particles.

The results from assays with αTSHscFv-ferritin particles (Figure 14A) showed that both urea- and pH-preparations bound specifically to TSH, as the negative control, wild-type ferritin particles did not display significant fluorescence in the assay (Table 3). These data also indicated that most αTSHscFv fragments refolded properly on the ferritin surface, and disulfide bridges formed in the presence of the redox shuffling agent, enabling the binding of αTSHscFv-ferritin particles to TSH.

Table 3. TSH-binding ability of αTSHscFv-ferritin particles generated by the pH and urea denaturation-refolding methods.

-Fold dilution	Fluorescence (RFU)[a]		
	αTSHscFv-ferritin; pH method	αTSHscFv-ferritin; urea method	Negative control[b]
50	5954±714	30857±6316	906±311
250	1168±70	8504±826	

[a] RFU, Relative fluorescence units,
[b]Excess wild-type ferritin was used as a negative control not binding specifically to wells.

To determine the activity of CBP on the ferritin surface, particles were first associated with a fusion protein composed of calmodulin and αTSHscFv, followed by evaluation of TSH-binding ability (Figure 14B). Particles bound specifically to TSH, as neither CBP-ferritin alone nor αTSHscFv-calmodulin combined with wild-type ferritin yielded significant fluorescence signal (Table 4). It may be concluded that CBP was able to bind to calmodulin on the surface of ferritin particles and that particles combined with αTSH-calmodulin effectively bound TSH.

Table 4. Calmodulin-binding ability of CBP-ferritin particles generated using both urea and pH denaturation-refolding methods. Denatured inclusion bodies of αTSH-calmodulin were added to refolding reactions.

-Fold dilution	Fluorescence (RFU)[a]			
	CBP-ferritin• combined with αTSHscFv-calmodulin		Negative controls[b]	
	Urea method	pH method	CBP-ferritin	Wild-type ferritin• combined with αTSHscFv-calmodulin
50	17615±1161	18628±787	1509±401	1230±61
250	8720±1296	10482±2047	738±29	977±113
1000	4875±159	5125±579	545±38	844±197

[a]RFU, Relative fluorescence units
[b]CBP-ferritin alone and wild-type ferritin combined with αTSH-calmodulin were used as negative controls to evaluate the specificity of the CBP calmodulin-binding activity.

8.2.3 Loading of Eu^{3+}

The amount of Eu^{3+} in each particle was estimated by binding BCCP-ferritin to streptavidin-coated microtiter wells as in Figure 13B, and (without adding labeled streptavidin) then detecting the amount of particle-associated Eu^{3+}. The concentration of BCCP-ferritin was determined using a ferritin-specific immunoassay (Figure 13A). The calculated number of Eu^{3+} ions per particle varied from 20 to 150, depending on the batch, and was commonly 30.

8.3 Functionality of particles in bioaffinity assays

8.3.1 Particles as labels

Functionality of complete particles consisting of ferritin with binding molecules on the outer surface and label activity inside were tested in bioaffinity assays using particles as labels (Figure 15). Also, the stability of the system was examined.

The use of BCCP-ferritin particles as labels was shown with a bioaffinity assay detecting biotinylated antibodies (Figure 15A). The response curve was linear over a wide range of analyte concentration (Figure 19A). The requirement for BCCP-ferritin particles was small; one

liter of culture provided enough material for 1,200,000 bioaffinity reactions under these assay conditions.

Stability of Eu^{3+}-containing particles was shown after storage at room temperature for at least 18 months, under final production conditions and without stabilizing agents. Particles remained functional in the bioaffinity assay after this time, although the signal level was somewhat reduced (Figure 19B). Additionally, a strong Eu^{3+} chelator, diethylenetriamine penta-acetic acid (DTPA), extracted only some Eu^{3+} from freshly prepared BCCP-ferritin particles, but was unable to extract Eu^{3+} from particles stored for 18 months (Figure 19). This indicates that most association between Eu^{3+} and the particles was very stable, but freshly prepared particles probably contained some DTPA-extractable Eu^{3+} ions attached (for example) on the surface.

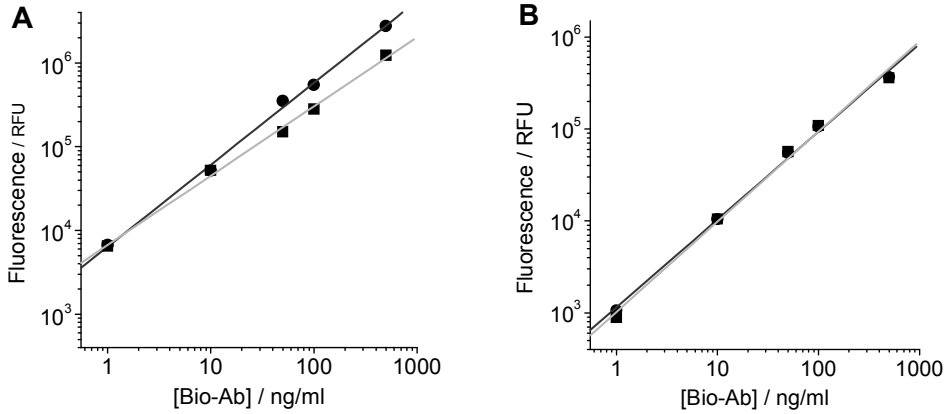

Figure 19. Use of BCCP-ferritin as label in a bioaffinity assay detecting a biotinylated molecule. Diethylenetriamine penta-acetic acid (DTPA), a strong chelator of Eu^{3+}, was used (at 0.5 mM) to test whether Eu^{3+} ions were loosely bound to the particles. Circles=without DTPA, squares=with DTPA. A. Functional BCCP-ferritin particles were obtained after particle formation. B. Particles were functional after 18 months of storage room temperature.

Complete functionalities of αTSHscFv-ferritin and CBP-ferritin particles loaded with Eu^{3+} ions were demonstrated in assays quantitatively detecting TSH (Figure 15B and C). Particles consisting of αTSHscFv-ferritin fusions generated by either the urea or pH denaturation-refolding methods effectively detected TSH in a concentration-dependent manner (Figure 20), and the dynamic range of the assay was 1,000-fold. The negative control, wild-type ferritin, produced and labeled as TSH-specific particles, did not display concentration dependency in the TSH assay. Application of excess DTPA, a strong chelator of Eu^{3+}, failed to remove Eu^{3+} ions from αTSH-ferritin produced by urea denaturation-refolding, confirmed by the finding that the assay fluorescence signal remained unaffected (Figure 20B). Thus, it appears that Eu^{3+} ions are an integral part of particles generated by the urea denaturation-refolding method, as with those obtained using the pH refolding method (Figure 19). These data confirmed the functionality of

particles with a protein fusion between a ferritin subunit and a single-chain antibody fragment, and using Eu^{3+} as a label.

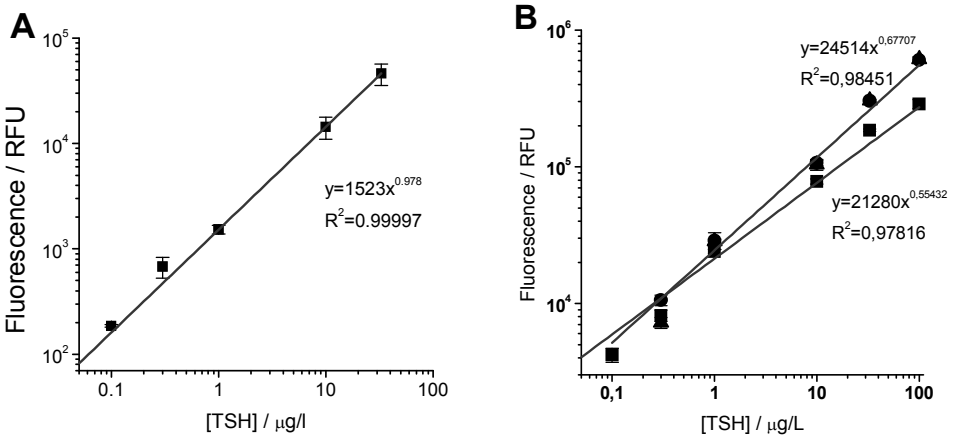

Figure 20. Bioaffinity assays for TSH using αTSHscFv-ferritin particles loaded with Eu^{3+} as label. Functionality of the particles is demonstrated by expression of TSH concentration-dependent signals. The means ± SDs (error bars) of three assays are presented. A. αTSHscFv-ferritin particles produced by the pH denaturation-refolding method. Squares=250-fold dilution of the particles. B. αTSHscFv-ferritin particles produced by the urea denaturation-refolding method, and using diethylenetriamine penta-acetic acid (DTPA), a chelator of Eu^{3+}, to examine whether weakly bound Eu^{3+} ions were associated with the particles. Circles=50-fold dilution, triagles=50-fold dilution with DTPA, Squares=250-fold dilution.

To show functionality of CBP-ferritin particles loaded with Eu^{3+}, particles were associated with αTSHscFv-calmodulin prior to TSH assay (Figure 15C). Concentration-dependent signals indicated that CBP-ferritin loaded with Eu^{3+} detected TSH (Figure 21). Both urea and pH denaturation-refolding methods were equally suitable for particle generation. Two methods of association of αTSHscFv-calmodulin with particles were studied. αTSHscFv-calmodulin was added either as a refolded protein to complete CBP-ferritin particles (Figure 21A) or as a denatured protein into the refolding reaction mixture (Figure 21B). Upon association of refolded αTSHscFv-calmodulin with complete CBP-ferritin particles, the standard curves (Figure 21A) were less steep than other curves (Figure 21B). It is possible that the calmodulin portion refolded more easily when CBP was present in refolding solution, or *vice versa*. The negative control (wild-type ferritin incubated with αTSHscFv-calmodulin) did not display any concentration-dependent signal.

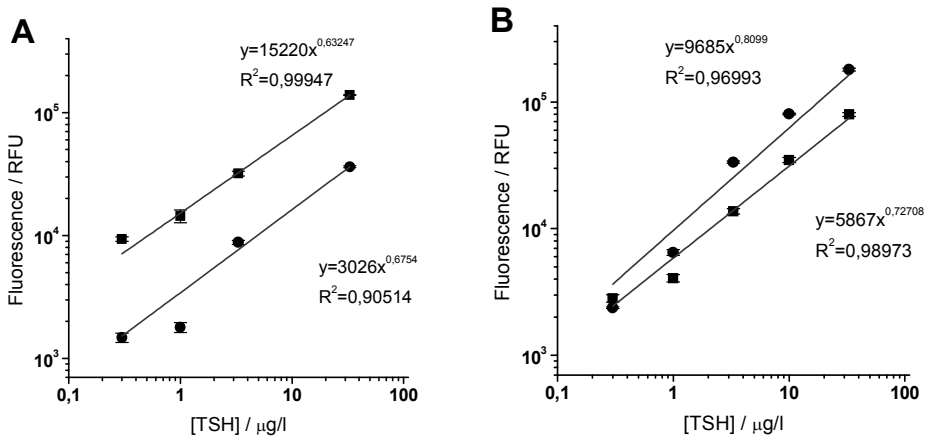

Figure 21. Bioaffinity assay for TSH using CBP-ferritin particles loaded with Eu^{3+} as label. Particles were linked to αTSHscFv-calmodulin molecules to enable binding to TSH. Particles produced by both urea and pH denaturation-refolding methods were used. The functionalities of the particles were assessed by generation of TSH concentration-dependent fluorescence signals. Means ± SDs (error bars) of three assays are presented. Squares=pH, Circles=urea. A. αTSHscFv-calmodulin was combined with complete CBP-ferritin particles. B. αTSHscFv-calmodulin was added to refolding CBP-ferritin.

Soluble αTSHscFv-calmodulin derived from cell lysates, in addition to material obtained from inclusion bodies (Figure 22), was tested. Interestingly, it was possible to associate non-purified TSH-binding molecules from cell lysates with CBP-ferritin particles without losing TSH-binding activity. However, direct comparison of particle performance using lysate and inclusion body αTSHscFv-calmodulins was not possible, because the concentrations of αTSHscFv-calmodulin could not be precisely determined.

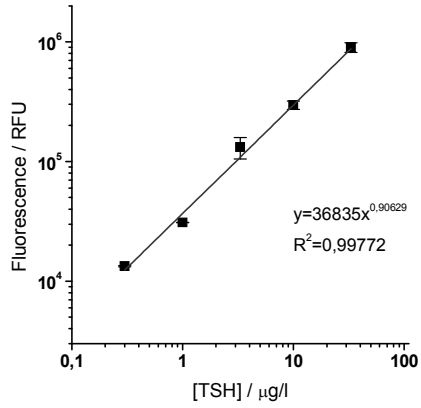

Figure 22. Bioaffinity assay for TSH using CBP-ferritin particles loaded with Eu^{3+} as the label (see Figure 15C). Particles were linked to αTSHscFv-calmodulin molecules to enable binding to TSH. Soluble αTSHscFv-calmodulin from a bacterial lysate was added to the refolding solution of CBP-ferritin. Particles produced by the pH refolding method were used. Particle functionalities were assessed by TSH concentration-dependent fluorescence signals. Means±SDs (error bars) of three reactions are presented.

8.3.2 Particles in particle-enhanced agglutination assays

We wished to establish whether the small (12 nm) ferritin particle body could be employed in particle-enhanced agglutination assays. BCCP-ferritin, with biotin on the surface, was used as a model particle because the target molecule, streptavidin, is able to agglutinate the particles because streptavidin possesses four binding sites for biotin (Figure 16).

Interactions between streptavidin and BCCP-ferritin were first analyzed by TEM. Figure 23A shows TEM images of particles in the absence of the target protein, streptavidin. BCCP-ferritin particles settled as a particle monolayer, and were covered by the negative stain solution, so that single particles were easily visualized. Figure 23B shows an agglutination reaction, in which the majority of the particles were agglutinated with streptavidin and largest absorption change would be expected. No free BCCP-particles were visible, and, because the aggregates could not settle as monolayers but rather as three-dimensional bundles, the negative stain laid excessively on the aggregates and therefore particles appeared relatively small and were difficult to identify. A reaction using a large excess of target protein resulted in almost all available binding sites being occupied by protein. This blocked agglutination of BCCP-ferritin particles by streptavidin, and the absorbance change would be thus lowered. BCCP-ferritin particle aggregates were visible, and, depending on the amount of negative stain that covered the proteins, free streptavidin and also streptavidin bound to BCCP-ferritin were occasionally visualized (Figure 23C).

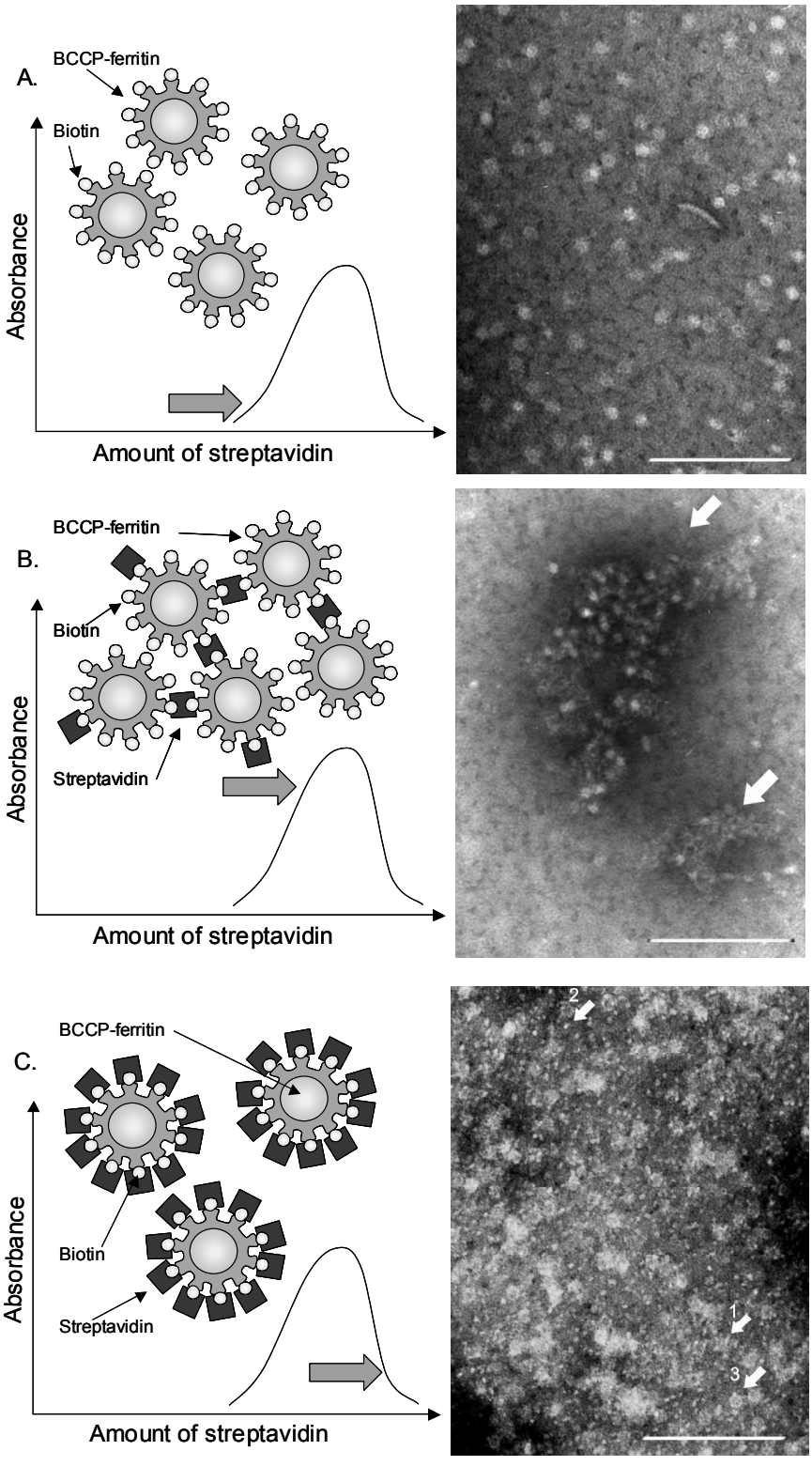
A.
BCCP-ferritin
Biotin
Absorbance
Amount of streptavidin
B.
BCCP-ferritin
Biotin
Streptavidin
Absorbance
Amount of streptavidin
C.
BCCP-ferritin
Biotin
Streptavidin
Absorbance
Amount of streptavidin
1
2
3

Figure 23. Agglutination reactions under different conditions. Samples were negatively stained with 0.5% (w/v) PTA. Scale bars represent 100 nm. A. BCCP-ferritin particles without the target protein, streptavidin. If the target protein was absent, there was no aggregation and the particle-containing solution showed no increase in absorbance (indicated by the arrow). Right panel: TEM image of BCCP-ferritin particles in the absence of streptavidin. B. BCCP-ferritin particles reacting with streptavidin. The number of biotin binding sites of streptavidin was roughly equivalent to the amount of biotin on BCCP-ferritin (*i.e.,* a 0.25 molar ratio of streptavidin molecules with respect to biotin on the ferritin surface). With an appropriate amount of streptavidin, specific agglutination of particles was achieved and the absorbance change was optimal (arrow). Right panel: TEM image of BCCP-ferritin particles specifically aggregated by streptavidin. A few aggregates were evident (white arrows), and the levels of free BCCP-ferritin or free streptavidin were negligible. C. BCCP-ferritin particles incubated with a large excess (10-fold) of streptavidin. In the presence of excess streptavidin, the majority of BCCP-ferritin particle binding sites were occupied by streptavidin, and specific particle agglutination was blocked, leading to a negligible rise in absorbance (indicated by arrow). Right panel: TEM image of BCCP-ferritin particles reacted with excess streptavidin showing individual BCCP-ferritin particles, with occasionally visualized bound streptavidin (white arrow #1). Free streptavidin can also be seen (white arrow #2), as can a few particles bound to each other (white arrow #3).

The agglutination of BCCP-ferritin particles with streptavidin was also examined spectrophotometrically (Figure 24). The absorption change produced by the specific reaction between streptavidin and BCCP-ferritin with surface biotin was confirmed by addition of excess free biotin before BCCP-ferritin particles were added. Free biotin blocked biotin-binding sites of streptavidin and prevented BCCP-ferritin binding to streptavidin. In the presence of free biotin the absorbance level did not increase when BCCP-ferritin particles were added (Figure 24B), indicating that free biotin blocked the biotin-binding sites of streptavidin, thereby inhibiting the agglutination of BCCP-ferritin particles. Thus, the observed absorption reaction was specific (Figure 24A).

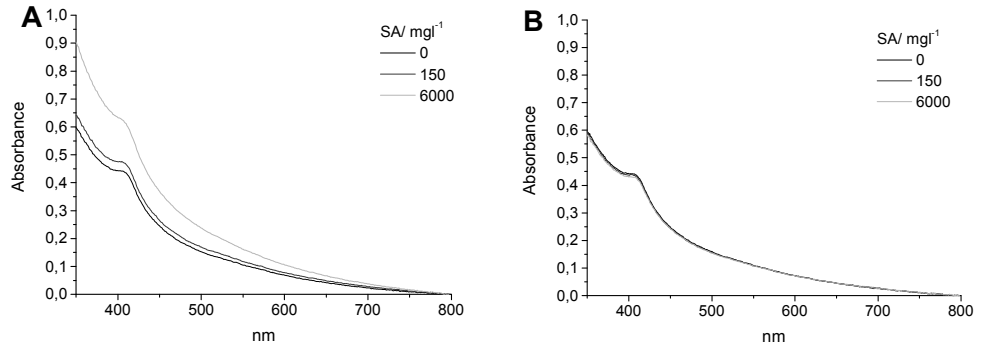

Figure 24. A. Absorption spectra of BCCP-ferritin (1.5 mg/ml) reacting with various amounts of streptavidin. B. Specificity of the agglutination was shown by adding free biotin before addition of streptavidin to the reaction. Absorbances between wavelengths 350 and 800 nm are shown.

Figure 25 shows streptavidin-dependent absorption changes generated by BCCP-ferritin particles at selected wavelengths; the absolute changes in absorbances are relatively small. This may be because of the relatively small amount of biotin on the ferritin surface. It is probable that BCCP is not adequately biotinylated when the protein is produced in inclusion bodies (Cronan, 1990). The results show, however, that ferritin-based particles can be used in particle-enhanced agglutination assays even though the particles are relatively small for the application.

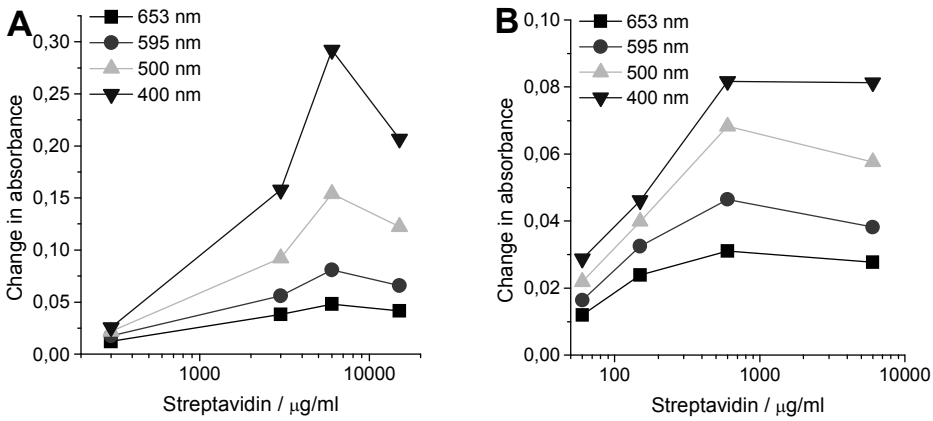

Figure 25. Particle-enhanced agglutination reactions between streptavidin and biologically produced and *in vivo* biotinylated BCCP-ferritin particles. BCCP-ferritin at (A) 1.5 mg/ml and (B) 0.3 mg/ml of BCCP-ferritin reacting with various amounts of streptavidin. Absorbances at wavelengths 400, 500, 595, and 635 nm are shown.

9 Conclusions and future prospects

In conclusion, synthesis of BCCP-ferritin particles showed that it is possible to generate protein-based nanoparticles using a simple biological production system. These particles had specific binding and label activities, which enabled their use in biological assays measuring desired molecules. Two different assay types were described: a heterogeneous bioaffinity assay on a solid phase; and a homogeneous, separation-free, particle-enhanced agglutination assay.

The general worth of the system was demonstrated using two additional binding molecules, the αTSHscFv antibody fragment and CBP. The use of different binding moieties showed, as might be expected, that production and refolding conditions for different molecules need to be individually adjusted. Overall, such adjustment may be of value in effective particle formation.

This biological procedure for generation of functional particles is, to a large extent, a "green method", which is increasingly important also in nanotechnology applications as have been reviewed by Bhattacharya and Gupta (2005), Eckelman *et al.* (2008) and Sarikaya *et al.* (2003). The twelve principles of green chemistry are mainly followed (U.S. Environmental Protection Agency): (1) No toxic waste or waste to be treated is generated. (2) Particle body consists of biological molecule, ferritin, thus the produced material is biodegradable and it is not toxic. (3) Synthesis of the particles is not hazardous: safe raw materials are used and no hazardous side products are generated. (5) Bacterial cells are biocatalyst factories the enzymatic pathways of which can additionally be modified (Maury *et al.*, 2005). (6) Temporary chemical derivatives are not needed. (8) No organic solvents are used. (9) Bacterial material production saves energy: simple and inexpensive sugar is used as source of energy and bacterial fermentation can be performed in mild conditions. Also, the material of both particle body and binding moieties are co-produced and the whole procedure is simplified and shortened employing generic methods. Hence the overall energy requirements are reduced. (10) Protein is biodegradable and does not accumulate in environment. (12) The process is not hazardous (safe reagents, methods, products). Renewable raw materials (item 4) are mainly used with exception of Eu^{3+} ions, which needs to be mined. Items 7 and 11 of the principles of green chemistry do not apply to biological production.

In addition to green aspects, this biological procedure may have several advantages in nanoparticle production, particularly in applications that require mass production of homogeneous functional particles often and regularly. These make system suitable for industrial purposes. *First*, ready-to-use particles are produced from simple carbon raw material in a single bacterial culture, followed by straightforward purification instead of multiple distinct preparation steps. The whole process is even simpler than production of binding molecules used in traditional functionalization of nanoparticles. *Second*, production is cost-effective, because the total time required is brief, the materials used are generic and inexpensive, and only a relatively small amount of energy is needed. *Third*, the process is readily upscalable. *Fourth*, binding molecules are favorably oriented on the surface (binding sites point into solution) when compared to typical methods that lead to random orientation of the binding moieties. *Fifth*, the conjugation of the binding molecule by genetic fusion is stable because the binding moiety is

covalently connected to the particle. This means that there are no weakly bound binders that might interfere final applications. *Sixth*, and importantly, affinity reagents (peptides, recombinant antibodies, binder scaffolds) developed using in vitro display methods, such as phage or cell surface display (Lu *et al.*, 1995; Smith, 1985), can be easily combined with the production system presented here, enabling generation of labeled particles of virtually any antigen specificity.

These ferritin-based nanoparticles have properties that may make them valuable as label agents or nanoparticles in bioaffinity assays. *First*, the particles have inherent binding activity, good water solubility, and (likely) biocompatibility. The particles do not need extra modification and purification steps for ensuring water solubility as traditional organic and inorganic particles often need. *Second*, ferritin is stable. *Third*, the particles are uniform and small (< 20 nm in diameter), which minimizes steric hindrance when particles encounter target molecules. Generating small and structurally similar particles using traditional methods is still a challenge.

To estimate the actual commercial utility of these biological particles in bioaffinity assays, the particle performance with an optimized assay should be evaluated. Especially testing assays under true assay conditions (*e.g.*, using true sample matrixes) would be essential to ensure overall utility of the system.

Further research directions could include identifying the particle characteristics that possibly require further optimization. For example, refolding conditions could be explored further to improve the refolding of complex binding molecules. Also loading of Eu^{3+} should preferably be improved. A recently introduced method for generating Eu^{3+} oxide particles specifically within apoferritin using UV light might be useful. Formation of particles inside ferritin using high-oxidation state ions such as Eu^{3+} or Ti^{4+}, has not been previously successful (Klem *et al.*, 2008). However, used heat treatment (+65°C) might be challenging when certain complicated binding molecules on ferritin surface are required. Additionally, efficient lanthanide-binding peptides selected for binding of *e.g.,* Tb^{3+} or Eu^{3+} could be fused to C-terminal ends of ferritin and displayed inside the ferritin cage (Nitz *et al.*, 2003).

The range of applications incorporating these biologically produced particles could and should be expanded in future. For example, removal of metal ions that are not loaded inside ferritin is necessary for some nanoparticle applications (*e.g.*, homogeneous assays that employ labeled nanoparticles). A straightforward and easily upscalable procedure is attractive from the perspective of principles of green chemistry and economy. Methods based on precipitation of non-loaded ions could be helpful if co-precipitation of ferritin particles can be controlled. Additionally, the production procedure presented here is possibly compatible with several methods for loading different materials inside apoferritin (Table 1), which remarkably widens the possibilities using it. For example, synthesis of particles geared towards *in vivo* applications such as magnetic resonance imaging could be an interesting and viable goal.

10 Acknowledgements

The work was carried out in the Biotechnology Department of University of Turku. The financial support for the work from Finnish Funding Agency for Technology and Innovation (TEKES) is gratefully acknowledged.

Thank you, Professor Timo Lövgren for the possibility to work with my thesis in the department even after having moved on to other challenges. Thank you also for the support you have offered me in my career.

Reviewers of my thesis, Professor Pirkko Heikinheimo and Dr. Per Matsson: Thank you for your time and comments that have helped me to improve the manuscript.

~~~~~~

Marko, I really have no words ---- You have the vision!! And thank you for keeping me on board during these years with your unfailing and professional support!

~~~~~~

Thank you, my other supervisors for always having made the time to answer my questions and review all the papers and thesis; Professor Tero Soukka, thank you for sharing your knowledge, particularly in assay technologies. Professor Lauri J. Pelliniemi, thank you for your expertise in electron microscopy.

Thank you "Pronano" project and my co-writers: Maria Lahti, Professor Marko Virta, Pia Nikander, Reija-Riitta Harinen, Dr. Teemu Korpimäki, Professor Tero Soukka, Dr. Urpo Lamminmäki. Thank you, "Pronano" inventors for giving me opportunity to work in a project with such a lively subject. And thank you other co-workers for sharing everyday successes and problems in the past. All in all, we have had some good times, haven't we!

Thank you, all colleagues from the Biotechnology lab! Thank you for putting up with all my lab reagents, those "bulky" particles and assorted stuff in the lab through all this time. Special thanks to Mirja Jaala, Marja Maula, Pirjo Laaksonen and Martti Sointusalo for keeping the laboratory up! I want also to thank those people currently in the lab that I haven't had a chance to get to know in person – remember, no matter what they say, I'm not a ghost in an old ragged lab coat working in the weekends.

Thank you, staff of Laboratory of electron microscopy, Leena Salminen, Marja Huhtinen, Jenni Kangas, Björn Enberg, Jouko Mäki. The atmosphere in your lab has always been so refreshing and cozy. Your help and encouragement warms my heart every time I see you!

Thank you, Professor Matti Karp. You have really given a kick-start to my career. I am truly grateful for that!

Innotrac Diagnostics Oy: Thank you for giving me the opportunity to see to the other side of the biological science. Special thanks to Dr. Harri Takalo, you gave me the encouraging permission for continuing my thesis. Thank you, all co-workers for moments of delight (and of course, sweets!).

Then, the work for this thesis has taken quite a long time, and it has sometimes felt like never-ending. Therefore, I want to thank some essential people, without whom this might still be an ongoing process, or at least the "here and now" of my thesis would be different:

Thank you, Marja-Liisa Knuuti for the help with all complicated bureaucracy.

Thank you, my dear "librarians" (kirjastontädit), Elena, Manu, Siina, Suvi, Yura.

Thank you, Dr. Leena Kokko for some heavy-duty advice!

Thank you for all possible practical / theoretical / mental counsel and help for my thesis: Eeva-Christine Brockmann, Jarmo Rainaho, Dr. Jukka Hellman, Dr. Kaisa Hakkila, Markus Vehniäinen, Dr. Niko Meltola, Dr. Pauliina Niemelä, Pertti Tolonen, Piitu Jauria, Rina Wahlroos, Dr. Susann Eriksson, Tiina Kokko and Dr. Ville Santala.

Thank you, my occasional housekeeper, Yura.

Thank you, my occasional dogsitters, Äiti, Isi, Suvi.

Thank you for the efficient rational words in times of huge scientific desperation, Marko, Suvi.

Thank you, my entertainers, Kummeli, Matti&Teppo.

Thank you, my football (well… also beer) pals, Jarmo, Juha, Juri.

Thank you, my dissertation "kaasos", hedgehoggy princesses and dear friends, Paula (The regular hedgehog) and Sinikka (The long-eared, African hedgehog). Thank you for both essential practical help and hilarious moral support at all times!

Thank you, all my superfriends for all the fun times we have spent! Anne "Aha", Erik "Eetu", Hanna "Hande", Heidi "Heppa", Ilari "Ilsu", Jussi "Tsuusi", Katja "Ulla Jr.", Lotta "Lahti-Lotta", Noora M., Pia N., Raine "Rönee", Reija-Riitta "Reijo", Sanna G., Siina "Sipsi", Sirkku "Sirkkeli", Tiina "Tiiwii", Tiina "Kuopiontiina" and all others.

~~~~~~

And finally, my greatest thanks go to those who have always and for all my life wished the best for me. Your impact has been enormous! ***Suurin kiitos teille, jotka olette aina ja koko elämäni ajan toivoneet kaikkea parasta minulle: Isi, Äiti, Suvi, Mummi (†), Sanni, Sake, Pinksi. Teidän vaikutuksenne on ollut hirmuisen suuri!*** *My little sister Suvi (also a hedgehog), I'm lucky to have you as my sister and friend. I will always be there for you.*

Leevi, my sweet little hairy darling, you've kept me alive all these years! You have definitiely earned a canine PhD in biotechnology during the time we worked together on my thesis.

Yura, you are the happiness of my life.

Turku, April 2009
~~~~~~

11 References

Abe S, Niemeyer J, Abe M, Takezawa Y, Ueno T, Hikage T, Erker G, Watanabe Y. 2008. Control of the coordination structure of organometallic palladium complexes in an apo-ferritin cage. J Am Chem Soc 130(32):10512-4.

Ahn J-E, Choi H, Kim Y-H, Han K-Y, Park J-S, Han S-S, Lee J. 2005. Heterologous gene expression using self-assembled supra-molecules with high affinity for HSP70 chaperone. Nucleic Acids Res 33(12):3751-3762.

Aime S, Cabella C, Colombatto S, Geninatti Crich S, Gianolio E, Maggioni F. 2002a. Insights into the use of paramagnetic Gd(III) complexes in MR-molecular imaging investigations. J Magn Reson Imaging 16(4):394-406.

Aime S, Frullano L, Geninatti Crich S. 2002b. Compartmentalization of a gadolinium complex in the apoferritin cavity: a route to obtain high relaxivity contrast agents for magnetic resonance imaging. Angew Chem Int Ed Engl 41(6):1017-9.

Allen M, Willits D, Mosolf J, Young M, Douglas T. 2002. Protein cage constrained synthesis of ferrimagnetic iron oxide nanoparticles. Adv Mater 14(21):1562-1565.

Allen M, Willits D, Young M, Douglas T. 2003. Constrained synthesis of cobalt oxide nanomaterials in the 12-subunit protein cage from *Listeria innocua*. Inorg Chem 42(20):6300-5.

Andrews SC, Arosio P, Bottke W, Briat JF, von Darl M, Harrison PM, Laulhere JP, Levi S, Lobreaux S, Yewdall SJ. 1992. Structure, function, and evolution of ferritins. J Inorg Biochem 47(3-4):161-74.

Andrews SC, Smith JM, Yewdall SJ, Guest JR, Harrison PM. 1991. Bacterioferritins and ferritins are distantly related in evolution. Conservation of ferroxidase-centre residues. FEBS Lett 293(1-2):164-8.

Arosio P, Adelman TG, Drysdale JW. 1978. On ferritin heterogeneity. Further evidence for heteropolymers. J Biol Chem 253(12):4451-8.

Arosio P, Yokota M, Drysdale JW. 1977. Characterization of serum ferritin in iron overload: possible identity to natural apoferritin. Br J Haematol 36(2):199-207.

Atkinson MJ, Spanner MT, Rosemann M, Linzner U, Muller WA, Gossner W. 2005. Intracellular sequestration of 223Ra by the iron-storage protein ferritin. Radiat Res 164(2):230-3.

Banyard SH, Stammers DK, Harrison PM. 1978. Electron density map of apoferritin at 2.8-A resolution. Nature 271(5642):282-4.

Bennett KM, Zhou H, Sumner JP, Dodd SJ, Bouraoud N, Doi K, Star RA, Koretsky AP. 2008. MRI of the basement membrane using charged nanoparticles as contrast agents. Magn Reson Med 60(3):564-74.

Bhattacharya D, Gupta RK. 2005. Nanotechnology and potential of micro-organisms. Crit Rev Biotechnol 25(4):199-204.

Bird RE, Hardman KD, Jacobson JW, Johnson S, Kaufman BM, Lee SM, Lee T, Pope SH, Riordan GS, Whitlow M. 1988. Single-chain antigen-binding proteins. Science 242(4877):423-6.

Bou-Abdallah F, Biasiotto G, Arosio P, Chasteen ND. 2004. The putative "nucleation site" in human H-chain ferritin is not required for mineralization of the iron core. Biochemistry 43(14):4332-7.

Bozzi M, Mignogna G, Stefanini S, Barra D, Longhi C, Valenti P, Chiancone E. 1997. A novel non-heme iron-binding ferritin related to the DNA-binding proteins of the Dps family in Listeria innocua. J Biol Chem 272(6):3259-65.

Brockmann E-C, Cooper M, Strömsten N, Vehniäinen M, Saviranta P. 2005. Selecting for antibody scFv fragments with improved stability using phage display with denaturation under reducing conditions. J Immunol Methods 296(1-2):159-70.

Broxmeyer HE, Lu L, Bicknell DC, Williams DE, Cooper S, Levi S, Salfeld J, Arosio P. 1986. The influence of purified recombinant human heavy-subunit and light-subunit ferritins on colony formation in vitro by granulocyte-macrophage and erythroid progenitor cells. Blood 68(6):1257-63.

Bulte JW, Douglas T, Mann S, Frankel RB, Moskowitz BM, Brooks RA, Baumgarner CD, Vymazal J, Frank JA. 1994a. Magnetoferritin. Biomineralization as a novel molecular approach in the design of iron-oxide-based magnetic resonance contrast agents. Invest Radiol 29 Suppl 2:S214-6.

Bulte JW, Douglas T, Mann S, Frankel RB, Moskowitz BM, Brooks RA, Baumgarner CD, Vymazal J, Strub MP, Frank JA. 1994b. Magnetoferritin: characterization of a novel superparamagnetic MR contrast agent. J Magn Reson Imaging 4(3):497-505.

Butts CA, Swift J, Kang SG, Di Costanzo L, Christianson DW, Saven JG, Dmochowski IJ. 2008. Directing Noble Metal Ion Chemistry within a Designed Ferritin Protein. Biochemistry 47(48):12729-12739.

Ceci P, Ilari A, Falvo E, Chiancone E. 2003. The Dps protein of Agrobacterium tumefaciens does not bind to DNA but protects it toward oxidative cleavage: x-ray crystal structure, iron binding, and hydroxyl-radical scavenging properties. J Biol Chem 278(22):20319-26.

Chan WCW, Nie S. 1998. Quantum dot bioconjugates for ultrasensitie nonisotopic detection. Science 281(5385):2016-2018.

Chang MC, Keasling JD. 2006. Production of isoprenoid pharmaceuticals by engineered microbes. Nat Chem Biol 2(12):674-81.

Chasteen ND, Theil EC. 1982. Iron binding by horse spleen apoferritin. A vanadyl(IV) EPR spin probe study. J Biol Chem 257(13):7672-7.

Chen Y, Cho J, Young A, Taton TA. 2007. Enhanced stability and bioconjugation of photo-cross-linked polystyrene-shell, Au-core nanoparticles. Langmuir 23(14):7491-7.

Cheng YG, Chasteen ND. 1991. Role of phosphate in initial iron deposition in apoferritin. Biochemistry 30(11):2947-53.

Choi H, Ahn JY, Sim SJ, Lee J. 2005. Glutamate decarboxylase-derived IDDM autoantigens displayed on self-assembled protein nanoparticles. Biochem Biophys Res Commun 327(2):604-8.

Cozzi A, Santambrogio P, Levi S, Arosio P. 1990. Iron detoxifying activity of ferritin. Effects of H and L human apoferritins on lipid peroxidation in vitro. FEBS Lett 277(1-2):119-22.

Crichton RR, Bryce CF. 1973. Subunit interactions in horse spleen apoferritin. Dissociation by extremes of pH. Biochem J 133(2):289-99.

Crichton RR, Millar JA, Cumming RL, Bryce CF. 1973. The organ-specificity of ferritin in human and horse liver and spleen. Biochem J 131(1):51-9.

Cronan JE, Jr. 1990. Biotination of proteins in vivo. A post-translational modification to label, purify, and study proteins. J Biol Chem 265(18):10327-33.

Cutler C, Bravo A, Ray AD, Watt RK. 2005. Iron loading into ferritin can be stimulated or inhibited by the presence of cations and anions: a specific role for phosphate. J Inorg Biochem 99(12):2270-5.

Danon D, Goldstein L, Marikovsky Y, Skutelsky E. 1972. Use of cationized ferritin as a label of negative charges on cell surfaces. J Ultrastruct Res 38(5):500-10.

Dominguez-Vera JM, Colacio E. 2003. Nanoparticles of Prussian blue ferritin: a new route for obtaining nanomaterials. Inorg Chem 42(22):6983-5.

Dominguez-Vera JM, Gálvez N, Sánchez P, Mota AJ, Trasobares S, Hernández JC, Calvino JJ. 2007. Size-controlled water soluble Ag nanoparticles. Eur J Inorg Chem(30):4823-4826.

Douglas T, Dickson DP, Betteridge S, Charnock J, Garner CD, Mann S. 1995. Synthesis and Structure of an Iron(III) Sulfide-Ferritin Bioinorganic Nanocomposite. Science 269(5220):54-57.

Douglas T, Ripoll DR. 1998. Calculated electrostatic gradients in recombinant human H-chain ferritin. Protein Sci 7(5):1083-91.

Douglas T, Stark VT. 2000. Nanophase cobalt oxyhydroxide mineral synthesized within the protein cage of ferritin. Inorg Chem 39(8):1828-30.

Douglas T, Young M. 1998. Host-guest encapsulation of materials by assembled virus protein cages. Nature 393:152-155.

Dubertret B, Skourides P, Norris DJ, Noireaux V, Brivanlou AH, Libchaber A. 2002. In vivo imaging of quantum dots encapsulated in phospholipid micelles. Science 298(5599):1759-62.

Eckelman MJ, Zimmerman JB, Anastas PT. 2008. Toward green nano: E-factor analysis of several nanomaterial syntheses. J. Ind. Ecol. 12(3):316-28.

Ensign D, Young M, Douglas T. 2004. Photocatalytic synthesis of copper colloids from CuII by the ferrihydrite core of ferritin. Inorg Chem 43(11):3441-6.

Fargion S, Arosio P, Fracanzani AL, Cislaghi V, Levi S, Cozzi A, Piperno A, Fiorelli G. 1988. Characteristics and expression of binding sites specific for ferritin H-chain on human cell lines. Blood 71(3):753-7.

Fernandez B, Galvez N, Sanchez P, Cuesta R, Bermejo R, Dominguez-Vera JM. 2008. Fluorescence resonance energy transfer in ferritin labeled with multiple fluorescent dyes. J Biol Inorg Chem 13(3):349-55.

Fernandez B, Galvez N, Sanchez P, Morales J, Santoyo F, Cuesta R, Dominguez-Vera JM. 2007. Red and blue ferritin nanomagnets by dye-labeling to the protein shell. Inorg Chim Acta 360:3951-3954.

Flenniken M, Willits DA, Brumfield S, Young MJ, Douglas T. 2003. The small heat shock protein cage from Methanococcus jannaschii is a versatile nanoscale platform for genetic and chemical modification. Nano Lett 3(11):1573-1576.

Ford GC, Harrison PM, Rice DW, Smith JM, Treffry A, White JL, Yariv J. 1984. Ferritin: design and formation of an iron-storage molecule. Philos Trans R Soc Lond B Biol Sci 304(1121):551-65.

Galvez N, Sanchez P, Dominguez-Vera JM. 2005. Preparation of Cu and CuFe Prussian Blue derivative nanoparticles using the apoferritin cavity as nanoreactor. Dalton Trans(15):2492-4.

Galvez N, Sanchez P, Dominguez-Vera JM, Soriano-Protillo A, Clemente-Leon M, Coronado E. 2006. Apoferritin-encapsulated Ni and Co superparamagnetic nanoparticles. J Mater Chem 16:2757-2761.

Geninatti Crich S, Bussolati B, Tei L, Grange C, Esposito G, Lanzardo S, Camussi G, Aime S. 2006. Magnetic resonance visualization of tumor angiogenesis by targeting neural cell adhesion molecules with the highly sensitive gadolinium-loaded apoferritin probe. Cancer Res 66(18):9196-9201.

Gerl M, Jaenicke R, Smith JM, Harrison PM. 1988. Self-assembly of apoferritin from horse spleen after reversible chemical modification with 2,3-dimethylmaleic anhydride. Biochemistry 27(11):4089-96.

Gider S, Awschalom DD, Douglas T, Mann S, Chaparala M. 1995. Classical and quantum magnetic phenomena in natural and artificial ferritin proteins. Science 268(5207):77-80.

Grace JE, Jr., Van Eden ME, Aust SD. 2000. Production of recombinant human apoferritin heteromers. Arch Biochem Biophys 384(1):116-22.

Grady JK, Shao J, Arosio P, Santambrogio P, Chasteen ND. 2000. Vanadyl(IV) binding to mammalian ferritins. An EPR study aided by site-directed mutagenesis. J Inorg Biochem 80(1-2):107-13.

Hainfeld JF. 1992. Uranium-loaded apoferritin with antibodies attached: molecular design for uranium neutron-capture therapy. Proc Natl Acad Sci U S A 89(22):11064-8.

Harrison PM, Fischbach FA, Hoy TG, Haggis GH. 1967. Ferric oxyhydroxide core of ferritin. Nature 216(5121):1188-90.

Hayashi T, Sano K, Shiba K, Kumashiro Y, Iwahori K, Yamashita I, Hara M. 2006. Mechanism underlying specificity of proteins targeting inorganic materials. Nano Lett 6(3):515-9.

Hemmilä I, Mukkala V. 2001. Time-resolution in fluorometry technologies, labels, and applications in bioanalytical assays. Crit Rev Clin Lab Sci 38(6):441-519.

Hempstead PD, Yewdall SJ, Fernie AR, Lawson DM, Artymiuk PJ, Rice DW, Ford GC, Harrison PM. 1997. Comparison of the three-dimensional structures of recombinant human H and horse L ferritins at high resolution. J Mol Biol 268(2):424-48.

Hennequin B, Turyanska L, Ben T, Beltran AM, Molina SI, Li M, Mann S, Patane A, Thomas NR. 2008. Aqueous near-infrared fluorescent composites based on apoferritin-encapsulated PbS quantum dots. Adv Mater 20:3592-3596.

Hoare RJ, Harrison PM, Hoy TG. 1975. Structure of horse-spleen apoferritin at 6 angstom resolution. Nature 255(5510):653-4.

Hoppler M, Meile L, Walczyk T. 2008. Biosynthesis, isolation and characterization of 57Fe-enriched Phaseolus vulgaris ferritin after heterologous expression in *Escherichia coli*. Anal Bioanal Chem 390(1):53-9.

Hosein HA, Strongin DR, Allen M, Douglas T. 2004. Iron and cobalt oxide and metallic nanoparticles prepared from ferritin. Langmuir 20(23):10283-7.

Huh YS, Kim IH. 2003. Purification of fusion ferritin from recombinant *E. coli* using two-step sonications. Biotechnol Lett 25(12):993-6.

Huhtinen P, Kivelä M, Kuronen O, Hagren V, Takalo H, Tenhu H, Lövgren T, Härmä H. 2005. Synthesis, characterization, and application of Eu(III), Tb(III), Sm(III), and Dy(III) lanthanide chelate nanoparticle labels. Anal Chem 77(8):2643-8.

Härmä H, Soukka T, Lövgren T. 2001. Europium nanoparticles and time-resolved fluorescence for ultrasensitive detection of prostate-specific antigen. Clin Chem 47(3):561-8.

Ilari A, Stefanini S, Chiancone E, Tsernoglou D. 2000. The dodecameric ferritin from *Listeria innocua* contains a novel intersubunit iron-binding site. Nat Struct Biol 7(1):38-43.

Ingrassia R, Gerardi G, Biasiotto G, Arosio P. 2006. Mutations of ferritin H chain C-terminus produced by nucleotide insertions have altered stability and functional properties. J Biochem 139(5):881-5.

Iwahori K, Enomoto T, Furusho H, Miura A, Nishio K, Mishima Y, Yamashita I. 2007. Cadmium sulfide nanoparticle synthesis in Dps protein from *Listeria innocua*. Chem Mater 19:3105-3111.

Iwahori K, Morioka T, Yamashita I. 2006. The optimization of CdSe nanoparticles synthesis in the apoferritin cavity. Phys Status Solidi 203(11):2658-2661.

Iwahori K, Yoshizawa K, Muraoka M, Yamashita I. 2005. Fabrication of ZnSe nanoparticles in the apoferritin cavity by designing a slow chemical reaction system. Inorg Chem 44(18):6393-400.

Jappelli R, Cesareni G. 1996. Loop mutations affect ferritin solubility causing non-native aggregation of subunits or precipitation of fully assembled polymers. FEBS Lett 394(3):311-5.

Jappelli R, Luzzago A, Tataseo P, Pernice I, Cesareni G. 1992. Loop mutations can cause a substantial conformational change in the carboxy terminus of the ferritin protein. J Mol Biol 227(2):532-43.

Kadir FHA, Al-Massad FK, Fatemi SJA, Singh HK, Wilson MT, Moore GR. 1991. Electron transfer between horse ferritin and ferrihaemoproteins. Biochem J 278:817-820.

Katz E, Willner I. 2004. Integrated nanoparticle-biomolecule hybrid systems: synthesis, properties, and applications. Angew Chem Int Ed Engl 43(45):6042-108.

Kim HJ, Kim HM, Kim JH, Ryu KS, Park SM, Jahng KY, Yang MS, Kim DH. 2003. Expression of heteropolymeric ferritin improves iron storage in *Saccharomyces cerevisiae*. Appl Environ Microbiol 69(4):1999-2005.

Kim I, Hosein HA, Strongin DR, Douglas T. 2002. Photochemical reactivity of ferritin for CR(VI) reduction. Chem Mater 14:4874-4879.

Kim JW, Choi SH, Lillehei PT, Chu SH, King GC, Watt GD. 2005. Cobalt oxide hollow nanoparticles derived by bio-templating. Chem Commun (Camb)(32):4101-3.

Kim SW, Kim YH, Lee J. 2001. Thermal stability of human ferritin: concentration dependence and enhanced stability of an N-terminal fusion mutant. Biochem Biophys Res Commun 289(1):125-9.

Klem MT, Mosolf J, Young M, Douglas T. 2008. Photochemical mineralization of europium, titanium, and iron oxyhydroxide nanoparticles in the ferritin protein cage. Inorg Chem 47(7):2237-9.

Klem MT, Resnick DA, Gilmore K, Young M, Idzerda YU, Douglas T. 2007. Synthetic control over magnetic moment and exchange bias in all-oxide materials encapsulated within a spherical protein cage. J Am Chem Soc 129(1):197-201.

Klem MT, Willits D, Solis DJ, Belcher AM, Young M, Douglas T. 2005. Bio-inspired synthesis of protein-encapsulated CoPt nanoparticles. Adv Funct Mater 15:1489-1494.

Kramer RM, Li C, Carter DC, Stone MO, Naik RR. 2004. Engineered protein cages for nanomaterial synthesis. J Am Chem Soc 126(41):13282-6.

Kramer RM, Sowards LA, Pender MJ, Stone MO, Naik RR. 2005. Constrained iron catalysts for single-walled carbon nanotube growth. Langmuir 21(18):8466-70.

Lawson DM, Artymiuk PJ, Yewdall SJ, Smith JM, Livingstone JC, Treffry A, Luzzago A, Levi S, Arosio P, Cesareni G and others. 1991. Solving the structure of human H ferritin by genetically engineering intermolecular crystal contacts. Nature 349(6309):541-4.

Lawson DM, Treffry A, Artymiuk PJ, Harrison PM, Yewdall SJ, Luzzago A, Cesareni G, Levi S, Arosio P. 1989. Identification of the ferroxidase centre in ferritin. FEBS Lett 254(1-2):207-10.

Lee SH, Lee H, Park JS, Choi H, Han KY, Seo HS, Ahn KY, Han SS, Cho Y, Lee KH and others. 2007. A novel approach to ultrasensitive diagnosis using supramolecular protein nanoparticles. Faseb J 21(7):1324-34.

Lee SW, Mao C, Flynn CE, Belcher AM. 2002. Ordering of quantum dots using genetically engineered viruses. Science 296(5569):892-5.

Levi S, Cesareni G, Arosio P, Lorenzetti R, Soria M, Sollazzo M, Albertini A, Cortese R. 1987. Characterization of human ferritin H chain synthetized in *Escherichia coli*. Gene 51(2-3):269-74.

Levi S, Corsi B, Rovida E, Cozzi A, Santambrogio P, Albertini A, Arosio P. 1994a. Construction of a ferroxidase center in human ferritin L-chain. J Biol Chem 269(48):30334-9.

Levi S, Cozzi A, Arosio P. 2005. Neuroferritinopathy: a neurodegenerative disorder associated with L-ferritin mutation. Best Pract Res Clin Haematol 18(2):265-76.

Levi S, Luzzago A, Cesareni G, Cozzi A, Franceschinelli F, Albertini A, Arosio P. 1988. Mechanism of ferritin iron uptake: activity of the H-chain and deletion mapping of the ferro-oxidase site. A study of iron uptake and ferro-oxidase activity of human liver, recombinant H-chain ferritins, and of two H-chain deletion mutants. J Biol Chem 263(34):18086-92.

Levi S, Luzzago A, Franceschinelli F, Santambrogio P, Cesareni G, Arosio P. 1989a. Mutational analysis of the channel and loop sequences of human ferritin H-chain. Biochem J 264(2):381-8.

Levi S, Salfeld J, Franceschinelli F, Cozzi A, Dorner MH, Arosio P. 1989b. Expression and structural and functional properties of human ferritin L-chain from *Escherichia coli*. Biochemistry 28(12):5179-84.

Levi S, Santambrogio P, Cozzi A, Rovida E, Corsi B, Tamborini E, Spada S, Albertini A, Arosio P. 1994b. The role of the L-chain in ferritin iron incorporation. Studies of homo and heteropolymers. J Mol Biol 238(5):649-54.

Li M, Viravaidya C, Mann S. 2007. Polymer-mediated synthesis of ferritin-encapsulated inorganic nanoparticles. Small 3(9):1477-81.

Li M, Wong KKW, Mann S. 1999. Organization of inorganic nanoparticles using biotin-streptavidin connectors. Chem Mater 11:23-26.

Listowsky I, Blauer G, Enlard S, Betheil JJ. 1972. Denaturation of horse spleen ferritin in aqueous guanidinium chloride solutions. Biochemistry 11(11):2176-82.

Liu G, Lin Y. 2007. Electrochemical quantification of single-nucleotide polymorphisms using nanoparticle probes. J Am Chem Soc 129(34):10394-401.

Liu G, Wang J, Lea SA, Lin Y. 2006a. Bioassay labels based on apoferritin nanovehicles. Chembiochem 7(9):1315-9.

Liu G, Wang J, Wu H, Lin Y. 2006b. Versatile apoferritin nanoparticle labels for assay of protein. Anal Chem 78(21):7417-23.

Liu G, Wu H, Dohnalkova A, Lin Y. 2007. Apoferritin-templated synthesis of encoded metallic phosphate nanoparticle tags. Anal Chem 79(15):5614-9.

Liu G, Wu H, Wang J, Lin Y. 2006c. Apoferritin-templated synthesis of metal phosphate nanoparticle labels for electrochemical immunoassay. Small 2(10):1139-43.

Liu X, Jin W, Theil EC. 2003. Opening protein pores with chaotropes enhances Fe reduction and chelation of Fe from the ferritin biomineral. Proc Natl Acad Sci U S A 100(7):3653-8.

Lu Z, Murray KS, Van Cleave V, LaVallie ER, Stahl ML, McCoy JM. 1995. Expression of thioredoxin random peptide libraries on the Escherichia coli cell surface as functional fusions to flagellin: a system designed for exploring protein-protein interactions. Biotechnology (N Y) 13(4):366-72.

Luzzago A, Cesareni G. 1989. Isolation of point mutations that affect the folding of the H chain of human ferritin in *E.coli*. Embo J 8(2):569-76.

Macara IG, Hoy TG, Harrison PM. 1972. The formation of ferritin from apoferritin. Kinetics and mechanism of iron uptake. Biochem J 126(1):151-62.

Macara IG, Hoy TG, Harrison PM. 1973. The formation of ferritin from apoferritin. Inhibition and metal ion-binding studies. Biochem J 135(4):785-9.

Mann S, Bannister JV, Williams RJ. 1986. Structure and composition of ferritin cores isolated from human spleen, limpet (*Patella vulgata*) hemolymph and bacterial (*Pseudomonas aeruginosa*) cells. J Mol Biol 188(2):225-32.

Masala O, Seshadri R. 2004. Synthesis routes for large volumes of nanoparticles. Annu Rev Mater Res 34:41-81.

Matsuya T, Tashiro S, Hoshino N, Shibata N, Nagasaki Y, Kataoka K. 2003. A core-shell-type fluorescent nanosphere possessing reactive poly(ethylene glycol) tethered chains on the surface for zeptomole detection of protein in time-resolved fluorometric immunoassay. Anal Chem 75(22):6124-32.

Maury J, Asadollahi MA, Moller K, Clark A, Nielsen J. 2005. Microbial isoprenoid production: an example of green chemistry through metabolic engineering. Adv Biochem Eng Biotechnol 100:19-51.

Meldrum FC, Douglas T, Levi S, Arosio P, Mann S. 1995. Reconstitution of manganese oxide cores in horse spleen and recombinant ferritins. J Inorg Biochem 58(1):59-68.

Meldrum FC, Heywood BR, Mann S. 1992. Magnetoferritin: in vitro synthesis of a novel magnetic protein. Science 257(5069):522-3.

Meldrum FC, Wade VJ, Nimmo DL, Heywood BR, Mann S. 1991. Synthesis of inorganic nanophase materials in supramolecular protein cages. Nature 349:684-687.

Menshikova AY, Evseeva TG, Skurkis YO, Tennikova TB, Ivanchev SS. 2005. Monodisperse carboxylated polystyrene particles: syntheseis, electrokinetic and adsorptive properties. Polymer 46:1417-1425.

Neri D, de Lalla C, Petrul H, Neri P, Winter G. 1995. Calmodulin as a versatile tag for antibody fragments. Biotechnology (N Y) 13(4):373-7.

Niederer W. 1970. Ferritin: iron incorporation and iron release. Experientia 26(2):218-20.

Nikandrov VV, Gratzel CK, Moser JE, Gratzel M. 1997. Light induced redox reactions involving mammalian ferritin as photocatalyst. J Photochem Photobiol B 41(1-2):83-9.

Nitz M, Franz KJ, Maglathlin RL, Imperiali B. 2003. A powerful combinatorial screen to identify high-affinity terbium(III)-binding peptides. Chembiochem 4(4):272-6.

Okuda M, Iwahori K, Yamashita I, Yoshimura H. 2003. Fabrication of nickel and chromium nanoparticles using the protein cage of apoferritin. Biotechnol Bioeng 84(2):187-94.

Okuda M, Kobayashi Y, Suzuki K, Sonoda K, Kondoh T, Wagawa A, Kondo A, Yoshimura H. 2005. Self-organized inorganic nanoparticle arrays on protein lattices. Nano Lett 5(5):991-3.

Parker MJ, Allen MA, Ramsay B, Klem MT, Young M, Douglas T. 2008. Expanding the temperature range of biomimetic synthesis using a ferritin from the hyperthermophile *Pyrococcus furiosus*. Chem Mater 20(4):1541-1547.

Pead S, Durrant E, Webb B, Larsen C, Heaton D, Johnson J, Watt GD. 1995. Metal ion binding to apo, holo, and reconstituted horse spleen ferritin. J Inorg Biochem 59(1):15-27.

Polanams J, Ray AD, Watt RK. 2005. Nanophase iron phosphate, iron arsenate, iron vanadate, and iron molybdate minerals synthesized within the protein cage of ferritin. Inorg Chem 44(9):3203-9.

Price D, Joshi JG. 1982. Ferritin: a zinc detoxicant and a zinc ion donor. Proc Natl Acad Sci U S A 79(10):3116-9.

Price DJ, Joshi JG. 1983. Ferritin. Binding of beryllium and other divalent metal ions. J Biol Chem 258(18):10873-80.

Resnick DA, Gilmore K, Idzerda YU. 2006. Magnetic properties of Co3O4 nanoparticles mineralized in *Listeria innocua* Dps. J Appl Phys 99:08Q501.

Rice DW, Ford GC, White JL, Smith JMA, Harrison PM. 1983. The spatial structure of horse spleen apoferritin. Adv Inorg Biochem 5:39-50.

Rohrer JS, Islam QT, Watt GD, Sayers DE, Theil EC. 1990. Iron environment in ferritin with large amounts of phosphate, from *Azotobacter vinelandii* and horse spleen, analyzed using extended X-ray absorption fine structure (EXAFS). Biochemistry 29(1):259-64.

Rucker P, Torti FM, Torti SV. 1997. Recombinant ferritin: modulation of subunit stoichiometry in bacterial expression systems. Protein Eng 10(8):967-73.

Sano K, Ajima K, Iwahori K, Yudasaka M, Iijima S, Yamashita I, Shiba K. 2005. Endowing a ferritin-like cage protein with high affinity and selectivity for certain inorganic materials. Small 1(8-9):826-32.

Santambrogio P, Levi S, Arosio P, Palagi L, Vecchio G, Lawson DM, Yewdall SJ, Artymiuk PJ, Harrison PM, Jappelli R and others. 1992. Evidence that a salt bridge in the light chain contributes to the physical stability difference between heavy and light human ferritins. J Biol Chem 267(20):14077-83.

Santambrogio P, Levi S, Cozzi A, Corsi B, Arosio P. 1996. Evidence that the specificity of iron incorporation into homopolymers of human ferritin L- and H-chains is conferred by the nucleation and ferroxidase centres. Biochem J 314 (Pt 1):139-44.

Santambrogio P, Levi S, Cozzi A, Rovida E, Albertini A, Arosio P. 1993. Production and characterization of recombinant heteropolymers of human ferritin H and L chains. J Biol Chem 268(17):12744-8.

Santambrogio P, Pinto P, Levi S, Cozzi A, Rovida E, Albertini A, Artymiuk P, Harrison PM, Arosio P. 1997. Effects of modifications near the 2-, 3- and 4-fold symmetry axes on human ferritin renaturation. Biochem J 322 (Pt 2):461-8.

Sarikaya M, Tamerler C, Jen AK, Schulten K, Baneyx F. 2003. Molecular biomimetics: nanotechnology through biology. Nat Mater 2(9):577-85.

Schultz S, Smith DR, Mock JJ, Schultz DA. 2000. Single-target molecule detection with nonbleaching multicolor optical immunolabels. Proc Natl Acad Sci U S A 97(3):996-1001.

Sengonul M, Ruzicka J, Attygalle AB, Libera M. 2007. Surface modification of protein nanocontainers and their self-directing character in polymer blends. Polymer 48:3632-3640.

Sengupta A, Thai CK, Sastry MS, Matthaei JF, Schwartz DT, Davis EJ, Baneyx F. 2008. A genetic approach for controlling the binding and orientation of proteins on nanoparticles. Langmuir 24(5):2000-8.

Sharma H, Sharma SN, Kumar U, Singh VN, Mehta BR, Singh G, Shivaprasad SM, Kakkar R. 2008. Formation of water-soluble and biocompatible TOPO-capped CdSe quantum dots with efficient photoluminescence. J Mater Sci Mater Med.

Sidoli A, Tamborini E, Giuntini I, Levi S, Volonte G, Paini C, De Lalla C, Siccardi AG, Baralle FE, Galliani S and others. 1993. Cloning, expression, and immunological characterization of recombinant *Lolium perenne* allergen Lol p II. J Biol Chem 268(29):21819-25.

Simsek E, Kilic MA. 2005. Magic ferritin: A novel chemoterapeutic encapsulation bullet. J Magn Magn Mater 293:509-513.

Smith GP. 1985. Filamentous fusion phage: novel expression vectors that display cloned antigens on the virion surface. Science 228(4705):1315-7.

Smith JL. 2004. The physiological role of ferritin-like compounds in bacteria. Crit Rev Microbiol 30(3):173-85.

Smith-Johannsen H, Drysdale JW. 1969. Reversible dissociation of ferritin and its subunits *in vitro*. Biochim Biophys Acta 194(1):43-9.

Soukka T, Härmä H, Paukkunen J, Lövgren T. 2001. Utilization of kinetically enhanced monovalent binding affinity by immunoassays based on multivalent nanoparticle-antibody bioconjugates. Anal Chem 73(10):2254-60.

St. Pierre TG, Chua-Anusorn W, Sipos P, Kron I, Webb J. 1993. Reaction of hydrogen sulfide with native horse spleen ferritin. Inorg Chem 32(20):4480-4482.

Stefanini S, Cavallo S, Wang CQ, Tataseo P, Vecchini P, Giartosio A, Chiancone E. 1996. Thermal stability of horse spleen apoferritin and human recombinant H apoferritin. Arch Biochem Biophys 325(1):58-64.

Stefanini S, Desideri A, Vecchini P, Drakenberg T, Chiancone E. 1989. Identification of the iron entry channels in apoferritin. Chemical modification and spectroscopic studies. Biochemistry 28(1):378-82.

Stefanini S, Vecchini P, Chiancone E. 1987. On the mechanism of horse spleen apoferritin assembly: a sedimentation velocity and circular dichroism study. Biochemistry 26(7):1831-7.

Stillman TJ, Hempstead PD, Artymiuk PJ, Andrews SC, Hudson AJ, Treffry A, Guest JR, Harrison PM. 2001. The high-resolution X-ray crystallographic structure of the ferritin (EcFtnA) of *Escherichia coli*; comparison with human H ferritin (HuHF) and the structures of the Fe(3+) and Zn(2+) derivatives. J Mol Biol 307(2):587-603.

Su M, Cavallo S, Stefanini S, Chiancone E, Chasteen ND. 2005. The so-called *Listeria innocua* ferritin is a Dps protein. Iron incorporation, detoxification, and DNA protection properties. Biochemistry 44(15):5572-8.

Sun S, Arosio P, Levi S, Chasteen ND. 1993. Ferroxidase kinetics of human liver apoferritin, recombinant H-chain apoferritin, and site-directed mutants. Biochemistry 32(36):9362-9.

Swift J, Wehbi WA, Kelly BD, Stowell XF, Saven JG, Dmochowski IJ. 2006. Design of functional ferritin-like proteins with hydrophobic cavities. J Am Chem Soc 128(20):6611-9.

Takagi D, Yamazaki A, Otsuka Y, Yoshimura H, Kobayashi Y, Homma Y. 2007. Gold-filled apo-ferritin for investigation of single-walled carbon nanotube growth on substrate. Chem Phys Lett 445:213-216.

Takagi H, Shi D, Ha Y, Allewell NM, Theil EC. 1998. Localized unfolding at the junction of three ferritin subunits. A mechanism for iron release? J Biol Chem 273(30):18685-8.

Towe KM, Bradley WF. 1967. Minearoligical constitution of colloidal "hydrous ferric oxides". J Colloid Interface Sci 24:384-392.

Treffry A, Bauminger ER, Hechel D, Hodson NW, Nowik I, Yewdall SJ, Harrison PM. 1993. Defining the roles of the threefold channels in iron uptake, iron oxidation and iron-core formation in ferritin: a study aided by site-directed mutagenesis. Biochem J 296 (Pt 3):721-8.

Treffry A, Harrison PM. 1978. Incorporation and release of inorganic phosphate in horse spleen ferritin. Biochem J 171(2):313-20.

Treffry A, Harrison PM. 1980. Metal-ion-binding sites and the role of the iron-core in iron(II) uptake by ferritin. Biochem Soc Trans 8(5):655-6.

Treffry A, Harrison PM. 1984. Spectroscopic studies on the binding of iron, terbium, and zinc by apoferritin. J Inorg Biochem 21(1):9-20.

Trikha J, Theil EC, Allewell NM. 1995. High resolution crystal structures of amphibian red-cell L ferritin: potential roles for structural plasticity and solvation in function. J Mol Biol 248(5):949-67.

Trikha J, Waldo GS, Lewandowski FA, Ha Y, Theil EC, Weber PC, Allewell NM. 1994. Crystallization and structural analysis of bullfrog red cell L-subunit ferritins. Proteins 18(2):107-18.

Uchida M, Flenniken ML, Allen M, Willits DA, Crowley BE, Brumfield S, Willis AF, Jackiw L, Jutila M, Young MJ and others. 2006. Targeting of cancer cells with ferrimagnetic ferritin cage nanoparticles. J Am Chem Soc 128(51):16626-33.

Uchida M, Klem M, Allen M, Suci P, Flenniken M, Gillitzer E, Varpness Z, Liepold L, Young M, Douglas T. 2007. Biological Containers: Protein Cages as Multifunctional Nanoplatforms. Adv Mater 19:1025-1042.

Uchida M, Terashima M, Cunningham CH, Suzuki Y, Willits DA, Willis AF, Yang PC, Tsao PS, McConnell MV, Young MJ and others. 2008. A human ferritin iron oxide nano-composite magnetic resonance contrast agent. Magn Reson Med 60(5):1073-81.

Ueno T, Suzuki M, Goto T, Matsumoto T, Nagayama K, Watanabe Y. 2004. Size-selective olefin hydrogenation by a Pd nanocluster provided in an apo-ferritin cage. Angew Chem Int Ed Engl 43(19):2527-30.

U.S. Environmental Protection Agency. Web pages 8.3.2009. http://www.epa.gov/greenchemistry/pubs/principles.html.

Wade VJ, Levi S, Arosio P, Treffry A, Harrison PM, Mann S. 1991. Influence of site-directed modifications on the formation of iron cores in ferritin. J Mol Biol 221(4):1443-52.

Van Wuytswinkel O, Savino G, Briat JF. 1995. Purification and characterization of recombinant pea-seed ferritins expressed in *Escherichia coli*: influence of N-terminus deletions on protein solubility and core formation in vitro. Biochem J 305 (Pt 1):253-61.

Wang J, Liu G, Merkoci A. 2003. Electrochemical coding technology for simultaneous detection of multiple DNA targets. J Am Chem Soc 125(11):3214-5.

Wang Z, Li C, Ellenburg M, Soistman E, Ruble J, Wright B, Ho JX, Carter DC. 2006. Structure of human ferritin L chain. Acta Crystallogr D Biol Crystallogr 62(Pt 7):800-6.

Wardeska JG, Viglione B, Chasteen ND. 1986. Metal ion complexes of apoferritin. Evidence for initial binding in the hydrophilic channels. J Biol Chem 261(15):6677-83.

Warne B, Kasyutich OI, Mayes EL, Wiggins JAL, Wong KKM. 2000. Self assembled nanoparticulate Co:Pt for data storage applications. IEEE Trans Magn 36(5):3009-3011.

Vasalatiy O, Zhao P, Zhang S, Aime S, Sherry AD. 2006. Catalytic effects of apoferritin interior surface residues on water proton exchange in lanthanide complexes. Contrast Media Mol Imaging 1(1):10-4.

Watt GD, Jacobs D, Frankel RB. 1988. Redox reactivity of bacterial and mammalian ferritin: is reductant entry into the ferritin interior a necessary step for iron release? Proc Natl Acad Sci U S A 85(20):7457-61.

Wauters M, Michelson AM, Crichton RR. 1978. Studies on the mechanism of ferritin formation. Superoxide dismutase, rapid kinetics and Cr3+ inhibition. FEBS Lett 91(2):276-80.

Webb B, Frame J, Zhao Z, Lee ML, Watt GD. 1994. Molecular entrapment of small molecules within the interior of horse spleen ferritin. Arch Biochem Biophys 309(1):178-83.

Whaley SR, English DS, Hu EL, Barbara PF, Belcher AM. 2000. Selection of peptides with semiconductor binding specificity for directed nanocrystal assembly. Nature 405(6787):665-8.

Vidal R, Miravalle L, Gao X, Barbeito AG, Baraibar MA, Hekmatyar SK, Widel M, Bansal N, Delisle MB, Ghetti B. 2008. Expression of a mutant form of the ferritin light chain gene induces neurodegeneration and iron overload in transgenic mice. J Neurosci 28(1):60-7.

Wiedenheft B, Mosolf J, Willits D, Yeager M, Dryden KA, Young M, Douglas T. 2005. An archaeal antioxidant: characterization of a Dps-like protein from *Sulfolobus solfataricus*. Proc Natl Acad Sci U S A 102(30):10551-6.

Wilchek M, Bayer EA. 1999. Foreword and introduction to the book (strept)avidin-biotin system. Biomol Eng 16(1-4):1-4.

von Darl M, Harrison PM, Bottke W. 1994. Expression in *Escherichia coli* of a secreted invertebrate ferritin. Eur J Biochem 222(2):367-76.

von Maltzahn G, Ren Y, Park JH, Min DH, Kotamraju VR, Jayakumar J, Fogal V, Sailor MJ, Ruoslahti E, Bhatia SN. 2008. In vivo tumor cell targeting with "click" nanoparticles. Bioconjug Chem 19(8):1570-8.

Wong KK, Colfen H, Whilton NT, Douglas T, Mann S. 1999. Synthesis and characterization of hydrophobic ferritin proteins. J Inorg Biochem 76(3-4):187-95.

Wong KKW, Douglas T, Gider S, Awschalom DD, Mann S. 1998. Biomimetic synthesis and characterization of magnetic proteins (magnetoferritin). Chem Mater 10(1):279-285.

Wong KKW, Mann S. 1996. Biomimetic synthesis of cadmium sulfide-ferritin nanocomposites. Adv Mater 8(11):928-932.

Wu H, Engelhard MH, Wang J, Fisher DR, Lin Y. 2008. Synthesis of lutetium phosphate-apoferritin core-shell nanoparticles for potential applications in radioimmunoimaging and radioimmunotherapy of cancers. J Mater Chem 18:1779-1783.

Xu B, Chasteen ND. 1991. Iron oxidation chemistry in ferritin. Increasing Fe/O2 stoichiometry during core formation. J Biol Chem 266(30):19965-70.

Yamashita I, Hayashi J, Hara M. 2004. Bio-template synthesis of uniform CdSe nanoparticles using cage-shaped protein, apoferritin. Chem Lett 33(9):1158-1159.

Yamashita I, Kirimura H, Okuda M, Nishio K, Sano K, Shiba K, Hayashi T, Hara M, Mishima Y. 2006. Selective nanoscale positioning of ferritin and nanoparticles by means of target-specific peptides. Small 2(10):1148-52.

Yan F, Zhang Y, Yuan HK, Gregas MK, Vo-Dinh T. 2008. Apoferritin protein cages: a novel drug nanocarrier for photodynamic therapy. Chem Commun (Camb)(38):4579-81.

Yang X, Chasteen ND. 1999. Ferroxidase activity of ferritin: effects of pH, buffer and Fe(II) and Fe(III) concentrations on Fe(II) autoxidation and ferroxidation. Biochem J 338 (Pt 3):615-8.

Yang Z, Wang X, Diao H, Zhang J, Li H, Sun H, Guo Z. 2007. Encapsulation of platinum anticancer drugs by apoferritin. Chem Commun (Camb)(33):3453-5.

Yariv J, Kalb AJ, Sperling R, Bauminger ER, Cohen SG, Ofer S. 1981. The composition and the structure of bacterioferritin of *Escherichia coli*. Biochem J 197(1):171-5.

Ye Z, Tan M, Wang G, Yuan J. 2005. Development of functionalized terbium fluorescent nanoparticles for antibody labeling and time-resolved fluoroimmunoassay application. Talanta 65(1):206-10.

Yoshizawa K, Iwahori K, Sugimoto K, Yamashita I. 2006. Fabrication of gold sulfide nanoparticles using the protein cage of apoferritin. Chem Lett 35(10):1192-1193.

Yoshizawa K, Mishima Y, Park SY, Heddle JG, Tame JR, Iwahori K, Kobayashi M, Yamashita I. 2007. Effect of N-terminal residues on the structural stability of recombinant horse L-chain apoferritin in an acidic environment. J Biochem 142(6):707-13.

Zaman Z, Verwilghen RL. 1981. Non-enzymic glycosylation of horse spleen and rat liver ferritins. Biochim Biophys Acta 669(2):120-4.

Zborowski M, Fuh CB, Green R, Baldwin NJ, Reddy S, Douglas T, Mann S, Chalmers JJ. 1996. Immunomagnetic isolation of magnetoferritin-labeled cells in a modified ferrograph. Cytometry 24(3):251-9.

Zhang L, Swift J, Butts CA, Yerubandi V, Dmochowski IJ. 2007. Structure and activity of apoferritin-stabilized gold nanoparticles. J Inorg Biochem 101(11-12):1719-29.

Zhao G, Bou-Abdallah F, Arosio P, Levi S, Janus-Chandler C, Chasteen ND. 2003. Multiple pathways for mineral core formation in mammalian apoferritin. The role of hydrogen peroxide. Biochemistry 42(10):3142-50.

Zijlmans HJ, Bonnet J, Burton J, Kardos K, Vail T, Niedbala RS, Tanke HJ. 1999. Detection of cell and tissue surface antigens using up-converting phosphors: a new reporter technology. Anal Biochem 267(1):30-6.